13.18 Volcanogenic Massive Sulfide Deposits

MD Hannington, University of Ottawa, Ottawa, ON, Canada

13.18.1 Introduction

Volcanogenic massive sulfide (VMS) deposits are stratiform or stratabound accumulations of base metal sulfides that formed on or near the seafloor by precipitation from 250 to 350 °C, dominantly seawater-derived hydrothermal fluids. They are an important subclass of the more general 'massive sulfide' deposits, which also includes sedimentary-exhalative massive sulfides. VMS deposits consist of >60% sulfide minerals, mainly pyrite and/or pyrrhotite, with variable amounts of Cu, Zn, and Pb sulfides (chalcopyrite, sphalerite, and galena) as the main ore minerals. Most deposits are characterized by internal metal zoning, with Cu-rich sulfides occurring dominantly at the base and Zn- or Pb-rich sulfides at the top or outer margins, reflecting temperature-dependent solubilities of the ore minerals in cooling hydrothermal fluids discharged onto the seafloor (Figure 1). The massive ore may be underlain by a vertically extensive network of Cu-rich veins and disseminated sulfides, referred to as the 'feeder zone' or 'stringer zone,' and by intensely altered rocks (i.e., the 'alteration pipe'). Proximal deposits are those that formed immediately above or adjacent to the discharge site, whereas distal deposits may have accumulated at some distance from the vents. Host strata are predominantly volcanic rocks, although the ores themselves may have been deposited in sediments that occur within the volcanic succession. The metals and reduced sulfur are considered to be mainly derived from leaching of the underlying volcanic rocks, with a potentially important contribution of metals from contemporaneous magmas. Some portion of the reduced sulfur may also have been derived from coeval seawater. The flow of hydrothermal fluids to the seafloor is driven by convective circulation above a deep heat source, most commonly a subvolcanic magma chamber, ~2 km below the seafloor (Figure 2). The most spectacular examples of this process are the presently active submarine hydrothermal vents or 'black smokers' that occur at modern mid-ocean ridges, submarine volcanic arcs, and in back-arc basins. Because ancient VMS formed by essentially the same geological and geochemical processes occurring on the ocean floor today, many parallels have been drawn between modern and ancient deposits.

The genetic link between seafloor volcanism and hydrothermal activity in a modern context was first articulated as an outgrowth of plate tectonic theory, about 20 years before the discovery of black smokers, although the notion of metallic mineral deposits forming at submarine volcanoes existed long before then (e.g., see Stanton, 1984). The current model was introduced in the late 1950s (Knight, 1957; Oftedahl, 1958; Stanton, 1955), and by 1965 a clear picture of the likely origin of VMS deposits at seafloor hydrothermal vents was established (Gilmour, 1965; Roscoe, 1965; Stanton, 1960). When black smoker sulfide deposits were discovered at mid-ocean ridges (Francheteau et al., 1979; Hekinian et al., 1980), many of the details of ore formation in the submarine environment were already known from the study of ancient VMS deposits. However, black smoker vents provided the first opportunity to sample hydrothermal fluids responsible for VMS formation. Until that time, the major characteristics of the hydrothermal fluids were inferred mainly from the study of the ore minerals and the alteration of the volcanic host rocks.

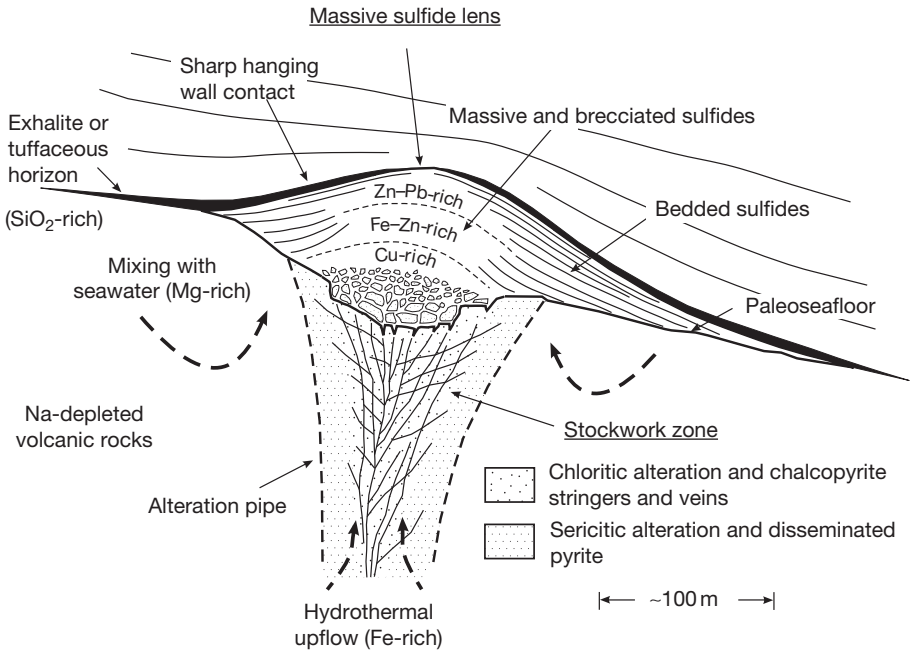

Figure 1 Schematic cross-section of a typical volcanogenic massive sulfide deposit. Adapted from Lydon JW (1984) Volcanogenic massive sulphide deposits Part I: A descriptive model. *Geoscience Canada* 11: 195–202.

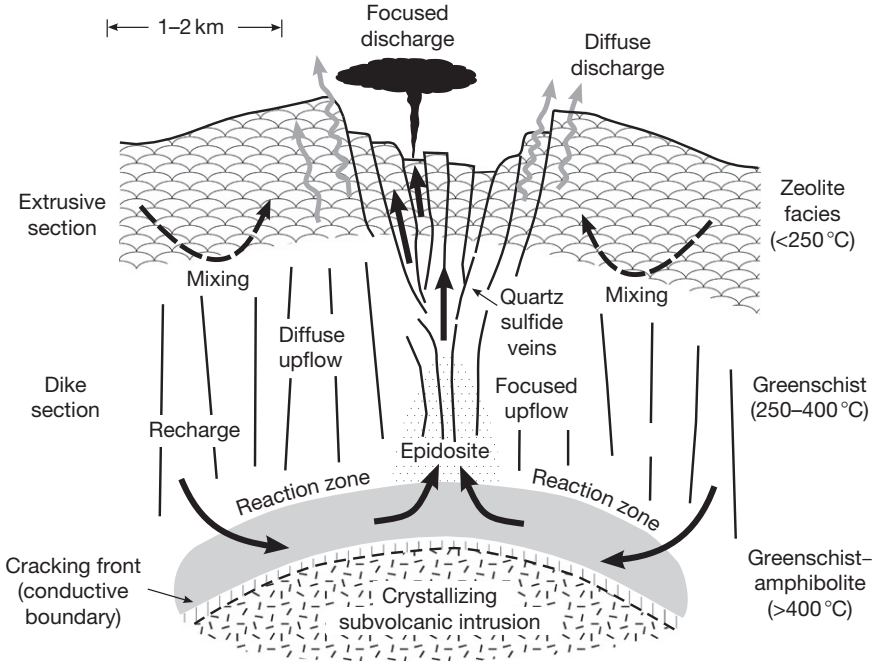

Figure 2 Model of typical submarine hydrothermal systems, illustrating the relationships between the reaction zone, upflow zone, and discharge zone. Approximate depths of the zeolite and greenschist facies metamorphic conditions and the greenschist–amphibolite transition are indicated. Adapted from Alt JC (1995) Subseafloor processes in mid-ocean ridge hydrothermal systems. In: Humphris SE, Zierenberg RA, Mullineaux LS, and Thomson RE (eds.) *Seafloor Hydrothermal Systems: Physical, Chemical, Biological, and Geological Interactions, Geophysical Monograph Series*, vol. 91, pp. 85–114. Washington, DC: American Geophysical Union.

This chapter focuses on the essential elements of the VMS genetic model as it pertains to the geochemistry of the deposits and the physical and chemical controls on ore deposition. These aspects were well established in early reviews by Large (1977), Franklin et al. (1981), Ohmoto et al. (1983), and Lydon (1984, 1988) and are revisited here with the benefit of new knowledge from the modern seafloor. The data from modern hydrothermal systems are now so much a part of the general genetic model for VMS deposits that it is difficult to separate our understanding of ancient deposits

from that of black smoker systems. For additional information on seafloor hydrothermal systems, interested readers are directed to German and Von Damm (2004).

13.18.2 Distribution, Abundance, and Classification

VMS deposits are among the oldest ore deposits on Earth, with examples in the Pilbara of Western Australia and the Barberton and Murchison greenstone belts of South Africa that date back to 3.45 billion years (Huston et al., 2010a). As a result, the fossil record of seafloor hydrothermal activity is impressive. More than 1000 deposits, ranging in size from a few hundred thousand to hundreds of millions of tonnes, have been mined or are included in the global geological resource (Franklin et al., 2005). Total past production, current reserves, and geological resources of VMS amount to nearly 14 billion tonnes; this includes 1200 M tonnes in the Archean, 2600 M tonnes in the Proterozoic, 8000 M tonnes in the Paleozoic, 1600 M tonnes in the Mesozoic, and 300 M tonnes in Cenozoic and younger rocks. Together, these deposits (and their close analogs, sedimentary-exhalative massive sulfide deposits) have accounted for more than half of global zinc and lead production, 7% of copper production, 18% of the silver, and a significant amount of gold and other by-product metals (Singer, 1995).

The deposits fall into two distinct groups based on metal content, a Cu–Zn group and a Zn–Pb–Cu group, which mainly reflect the compositions of the underlying volcanic rocks (Barrie and Hannington, 1999; Franklin et al., 1981; Large, 1992). Deposits of the Cu–Zn group are hosted by compositionally bimodal volcanic successions, dominated by mafic rocks but with felsic volcanic rocks commonly occurring in close association with the deposits. Deposits of the Zn–Pb–Cu group are in stratigraphic successions dominated either by felsic volcanic rocks or by subequal amounts of felsic volcanic and sedimentary strata. Comparisons with deposits in well-preserved volcanic terranes (e.g., Kuroko-, Cyprus-, and Besshi-type deposits, named after their type localities) have been the basis for interpreting the original geological settings of many ancient VMS systems. In the last 25 years, mapping of the seafloor also has allowed more precise tectonic classifications of VMS-hosting environments based on improved geodynamic models of submarine volcanic arcs, back-arc spreading centers, and mid-ocean ridges (Hannington et al., 2005). Franklin et al. (2005) applied these findings in their most recent review and classification of the major VMS districts worldwide, emphasizing the link between deposit type and lithostratigraphic association. Because VMS deposits form early in the development of orogenic belts, they also provide an important record of paleoenvironmental conditions and crustal evolution. For example, the preservation of compositionally different deposit types (e.g., with different Zn/Zn + Pb ratios) beginning in the Early Archean reflects the presence of crustal elements of different composition in the earliest history of the Earth.

Most Precambrian deposits formed during two relatively short intervals of crustal growth in the Late Archean (~2.7–2.75 Ga) and Early Proterozoic (~1.8 Ga). In Archean greenstone belts, the deposits formed mainly in oceanic rifts and primitive oceanic arc and back-arc systems; in the Paleoproterozoic, VMS formation occurred mainly during accretion of protocontinents and the development of major mobile belts. However, more than half of the total tonnage of VMS deposits discovered so far was formed during a brief 340 My period of arc and back-arc volcanism associated with subduction along Paleozoic continental margins of Australia, North America, and Europe (Appalachians, Tasman Geosyncline, North American Cordillera, Variscan fold belt of Spain and Portugal, and Uralian fold belt of Russia). VMS deposits in these metallogenic belts have many similarities to deposits currently forming on the seafloor, including Kuroko analogs in rifted island arcs of the western Pacific and Cyprus-type deposits at mid-ocean ridges and mature back-arc basin spreading centers. A widely accepted model for the tectonic setting of a majority of VMS deposits is an aborted arc rift, such as that proposed for the Miocene Kuroko deposits of Japan (Cathles et al., 1983). Major VMS districts in these settings share a common stratigraphic succession, beginning with arc-related submarine volcanism, followed by rapid extension and subsidence to deep marine conditions and back-arc spreading during which the deposits formed, and then a return to compression with closure and uplift of the basin. In many cases, a strip of back-arc crust is left attached to an aggregate of colliding arcs or caught between an active margin and a continent, thus preserving the contained massive sulfide deposits.

Felsic volcanic rocks are the immediate hosts for about half of all VMS deposits. Although this close link to bimodal basalt–rhyolite volcanism has been widely recognized, the small volumes of rhyolite associated with many deposits are unlikely to have been responsible for large-scale hydrothermal convection. Rather, the spatial association with felsic volcanic rocks most likely reflects anomalous heat flow during rifting and partial melting of basaltic crust, generating the small volumes of felsic magma (e.g., Lentz, 1998; Piercey, 2010). This may also explain why most VMS deposits are confined to relatively narrow stratigraphic intervals compared to the time span of volcanic activity in major arc–back-arc successions and why many large stratigraphic thicknesses of dominantly mafic submarine volcanic rocks are often devoid of such deposits. An alternative explanation is that ore formation is directly linked to fluids released from the felsic magmas. The deposits typically formed immediately after the cessation of volcanic activity or during depositional gaps or hiatuses in volcanism, which represent time periods when deep subvolcanic magma chambers were cooling and fractionating. The ore-related stratigraphic position is sometimes occupied by chemical sedimentary rocks (e.g., chert or oxide, silicate, and carbonate facies iron formation), which represent the distal products of hydrothermal discharge, or by laterally extensive laminated tuffaceous rocks. Where deposits occur at more than one stratigraphic horizon within a volcanic complex, multiple episodes of rifting and subvolcanic intrusive activity may have occurred.

13.18.3 Composition

All VMS deposits are polymetallic, consisting predominantly of iron sulfides, accompanied by sphalerite, chalcopyrite, and/or galena as the principal economic minerals. Iron sulfides typically constitute at least 30% the mined material. The ores

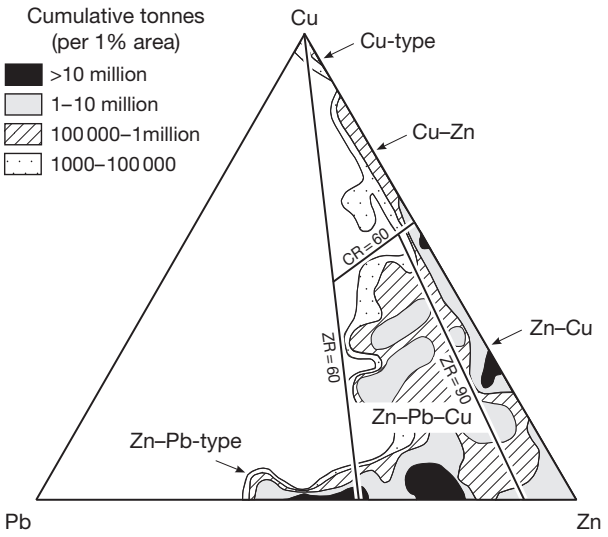

Figure 3 Range of compositions of VMS deposits. Contours indicate the proportional abundance of Cu, Zn, and Pb (tonnes per percent area of diagram; adapted from Franklin JM, Lydon JW, and Sangster DF (1981) Volcanic-associated massive sulfide deposits. In: Skinner BJ (ed.) *75th Anniversary Volume of Economic Geology*, pp. 485–627. Lancaster, PA: The Economic Geology Publishing Company). Compositional fields for Cu–Zn-type, Zn–Cu-type, and Zn–Pb–Cu-type deposits, based on zinc ratios (ZR = 100*Zn/(Zn + Pb)) and copper ratios (CR = 100*Cu/(Cu + Zn)), are adapted from Large RR (1992) Australian volcanic-hosted massive sulfide deposits: Features, styles, and genetic models. *Economic Geology* 87: 549–572.

range from massive pyritic or pyrrhotite-rich deposits with very low base metal contents (a few weight percent combined Cu + Zn + Pb) to very rich deposits. As noted above, high grades of Zn and Pb are most commonly associated with felsic volcanic and sedimentary successions, whereas Cu-rich pyritic deposits are commonly associated with mafic volcanic-dominated successions, and some Cu-rich deposits may have derived their metals directly from a felsic subvolcanic magma. Figure 3 shows the relative importance of the Cu-rich, Cu–Zn-rich, and Zn–Pb–Cu subgroups.

The close chemical affinity of VMS ores with their immediate host rocks, and especially the dominant lithology in the footwall (Table 1), supports the suggestion that the metals were derived, either by leaching in a convective hydrothermal system or by direct contributions from the parent magmas. Insofar as the tectonic environment influences the relative amounts of felsic and mafic volcanic rocks, the geodynamic setting is an important first-order control on the compositions of the deposits; some classification schemes have attempted to link the bulk compositions of VMS to their geodynamic environments. For example, the Cu-rich deposits found in ophiolite terranes, such as those in Cyprus and Oman, were long considered to be ancient analogs of modern black smokers on the mid-ocean ridges. Although there are remarkable similarities among the deposits, it is now understood that most ophiolites do not represent mid-ocean ridge crust but are mostly products of suprasubduction zone magmatism (Miyashiro, 1973; Pearce et al., 1981). Thus, the similarities between ophiolite-hosted massive sulfide deposits and modern black smokers mainly reflect the similar compositions of volcanic rocks in mature back-arc spreading centers and at mid-ocean ridges.

The proportions of metals in deposits hosted by mafic volcanic rocks closely match those of normal mid-ocean ridge basalt (N-MORB), whereas the proportions in deposits hosted by felsic volcanic rocks or sediment more closely match those of average continental crust (Figure 4). The contents of Cu and Au are similar for all deposit types, except those hosted by felsic siliciclastic rocks, which contain notably less Cu. Deposits hosted by volcaniclastic rocks or other sediments are also much larger, on average, than deposits in flow-dominated sequences (Table 1), reflecting the more effective trapping of metals by deposition within the more permeable host rocks. Cu-rich deposits are commonly enriched in trace elements such as Co, Se, Ni, and Bi (up to several hundreds of ppm), whereas Zn- and Pb-rich deposits commonly have high concentrations of Ag, As, Sb, and Hg. These and other elements occur in more than 100 different trace metallic minerals that are commonly found in VMS, including a wide range of sulfides, sulfosalts, oxides, and native elements (Table 2). The mean gold content of VMS deposits is low (<1 ppm), but a particular class of Au-rich VMS is also recognized (Mercier-Langevin et al., 2010). Factors that control the distribution of the trace elements in the ores are discussed further in Section 13.18.6.

The most common ore minerals (in decreasing order of abundance) are pyrite, chalcopyrite, sphalerite, and pyrrhotite, followed by minor amounts of galena, tetrahedrite, tennantite, arsenopyrite, bornite, and magnetite (Table 2). Pyrite is the predominant Fe sulfide in 75% of the deposits; pyrrhotite is more abundant in about 25% of the deposits. The sulfide minerals are typically very fine-grained, commonly having colloform and framboidal textures. Coarser-grained aggregates

Table 1 Geometric mean concentrations of metals in VMS ores according to host-rock type

	Mafic	*Bimodal mafic*	*Mafic–pelitic*	*Bimodal felsic*	*Felsic–siliciclastic*
Cu (wt%)	1.82	1.24	1.23	1.04	0.62
Zn (wt%)	0.84	2.32	1.58	4.36	2.70
Pb (wt%)	0.02	0.30	0.68	1.14	1.09
Au (ppm)	1.40	0.81	0.75	1.06	0.59
Ag (ppm)	11	21	19	56	39
Total ore (tonnes)	2 699 466	3 421 075	4 721 093	3 320 784	7 139 305
Total metal (tonnes)	63 035	128 515	132 968	198 461	324 748
N	76	291	90	241	106

Source: Franklin JM, Gibson HL, Jonasson IR, and Galley AG (2005) Volcanogenic massive sulfide deposits. In: Hedenquist JW, Thompson JFH, Goldfarb RJ, and Richards JP (eds.) *100th Anniversary Volume of Economical Geology*, pp. 523–560. Littleton, CO: Society of Economic Geologists.

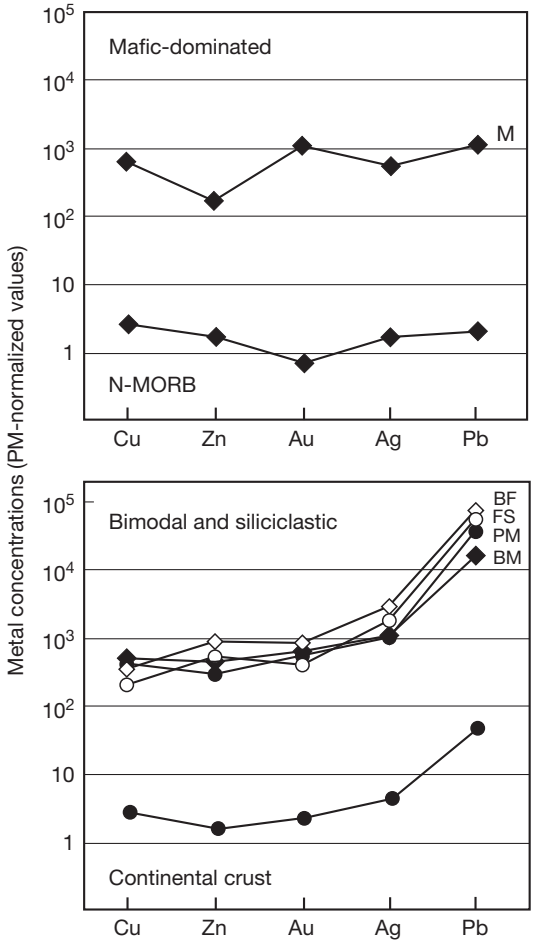

Figure 4 Primitive-mantle normalized values of average Cu, Zn, Au, Ag, and Pb concentration in different types of VMS deposits (**Table 1**), compared with those in N-MORB and average continental crust. Metal contents of deposits hosted by mafic volcanic rocks generally match the pattern for N-MORB, whereas those with a significant amount of felsic volcanic rocks (bottom panel) or sediment more closely match that of the average continental crust (primitive mantle values and average metal contents of N-MORB and continental crust from the compilation of Barrie and Hannington, 1999). M, mafic-dominated; BM, bimodal mafic; PM, pelitic mafic; BF, bimodal felsic; FS, felsic siliciclastic.

and granoblastic textures are typical of deposits that have been affected by later hydrothermal recrystallization, diagenesis, burial metamorphism, or deformation. Many deposits are recrystallized to such an extent that no primary textures are preserved at any scale, with different minerals and even entire ore lenses exhibiting ductile behavior during deformation according to the relative strengths of the sulfide minerals (e.g., pyrite > sphalerite = pyrrhotite > chalcopyrite > galena). These effects are considered in greater detail in **Chapter 13.7**.

Ore-related gangue minerals comprise 20–40% of the mined material. Quartz, muscovite, chlorite, barite, gypsum, and carbonate are the dominant ore-related gangue, although nearly 70 different nonsulfide minerals have been identified in the ores and altered host rocks. These minerals either coprecipitated with the sulfides from the ore-forming hydrothermal fluids or were formed by alteration of the volcanic and sedimentary host rocks and, in some cases, later metamorphism.

The bulk compositions of VMS deposits have changed over time. Phanerozoic VMS deposits have pyrite as the principal Fe sulfide, whereas most Precambrian massive sulfide deposits contain both pyrite and pyrrhotite in subequal amounts. This difference is interpreted to reflect the reduced bottom waters and lower total sulfur contents of the oceans that prevailed in the Archean and Early Proterozoic. Increasing concentrations of sulfate in seawater and more evolved crust are reflected by the abundant sulfate-rich gangue minerals and higher Pb contents, respectively, in Phanerozoic deposits. Barite is present locally in some of the oldest deposits, but it does not become widespread or abundant in VMS until after ~1.8 Ga, tracking the oxygenation of the late Precambrian oceans (Huston et al., 2010a).

13.18.4 General Genetic Model

VMS deposits are products of the hydrothermal convection of seawater, which is driven by oceanic crustal heat flow, especially above zones of recently crystallized or still molten magma (**Figure 2**). The ore-forming fluids originate from a series of high-temperature chemical reactions between seawater and volcanic rocks that produce a remarkably uniform solution containing metals and sulfur leached from the rocks

Table 2 Ore mineralogy of VMS deposits

Most abundant	*Second*	*Third*	*Fourth*	*Other trace minerals*
Pyrite (74)	Chalcopyrite (39)	Sphalerite (35)	Galena (28)	*Covellite*, *digenite*, gold, electrum,
Chalcopyrite (9)	Sphalerite (27)	Chalcopyrite (32)	Chalcopyrite (20)	silver, argentite, cubanite, bournonite,
Sphalerite (8)	Pyrrhotite (14)	Galena (12)	Pyrrhotite (7)	boulangerite, cobaltite, mackinawite,
Pyrrhotite (7)	Pyrite (11)	Pyrrhotite (9)	Magnetite (6)	stannite, cassiterite, bismuthinite,
Magnetite (<5)	Galena (<5)	Pyrite (5)	Pyrite (5)	bismuth, *limonite*, *copper*, *cuprite*,
Galena	Marcasite	Magnetite	Sphalerite	idaite, molybdenite, pentlandite,
Bornite	Bornite	Hematite	Hematite	tellurides, selenides, antimonides,
	Magnetite	Bornite	*Chalcocite*	Ag–Pb–As–Sb-sulfosalts
	Arsenopyrite	Tetrahedrite	Bornite	
	Enargite	*Chalcocite*	Arsenopyrite	
		Arsenopyrite	Tetrahedrite	
		Marcasite	Tennantite	

Numbers in brackets refer to the percentage of deposits in which the indicated mineral is the first, second, third, or fourth most abundant ore mineral. Other trace minerals are listed in approximate order of importance based on the number of deposits that contain the mineral. Based on data for 509 deposits in Mosier et al. (1983). Minerals in italics are mainly, although not exclusively, secondary in origin (i.e., supergene).

along the flow path. Hydrothermal circulation is most commonly localized by zones of active rifting or seafloor spreading where the crust above the magma is faulted and fissured, allowing seawater to penetrate to great depths (up to several kilometers) close to the heat source. Here, conductive heat transfer from the crystallizing top of the magma chamber draws cold seawater into the hydrothermal system. The depth, size, and shape of the heat source, and the extent of subseafloor fracturing control the scale of hydrothermal fluid flow and the temperature and pressure at which the hot water reacts with the surrounding rock (e.g., Cathles, 1997).

Reactions between heated seawater and the volcanic rocks occur first at low temperatures, as cold seawater is drawn into the crust in the down-flowing limb or 'recharge' zone of the hydrothermal convection cell, then at much higher temperatures in the deepest parts of the circulation system (the 'reaction' zone), and lastly as the superheated fluid rises through the 'upflow' zone to be discharged at the seafloor. Different reactions occur as the fluids are progressively heated, reaching equilibrium with the altered volcanic rocks in the reaction zone at a temperature of 400 °C . The pressures and temperatures in the reaction zone are controlled by density-driven fluid flow, with maximum hydrothermal convection occurring close to the critical point of seawater (407 °C and 298 bars; Bischoff and Rosenbauer, 1988; Kasting et al., 2006). After passing through the hottest part of the convective system, which may be solid rock or cooling magma, the hydrothermal solutions rise buoyantly along a zone of high permeability, commonly occupied by dikes that feed contemporaneous seafloor volcanic eruptions.

Subvolcanic intrusions are the dominant heat sources for the hydrothermal system. They are intruded to within a few kilometers of the seafloor, such as at actively spreading ridges, or are emplaced as larger intrusions in rifting arc crust or continental crust. Gabbro, diorite, tonalite, and trondhjemite are the most common types of subvolcanic intrusive rocks associated with VMS deposits, interpreted to be products of crustal melting within a high heat flow, extensional (rift) environment. The melting is most likely triggered by the rise of mantle-derived mafic melts into the upper crust (Hart et al., 2004; Lesher et al., 1986). Importantly, the subvolcanic intrusions are comagmatic with the host volcanic strata of the VMS deposits. The intrusions typically lack significant contact metamorphic aureoles, in part because of efficient heat transfer caused by hydrothermal cooling (e.g., Cathles et al., 1997). Instead, well-developed metasomatic zones, dominated by greenschist-to-lower amphibolite facies secondary minerals, occur both in the margins of the intrusions and may extend for hundreds of meters above the intrusions. Magmatic–hydrothermal mineral assemblages (e.g., quartz–epidote–amphibole-filled miarolitic cavities) also may develop within the intrusions, either as a product of interaction between the melt and seawater or from devolatilization of the rapidly cooled magmas (Galley, 2003). A number of features, including stable and radiogenic isotope tracers, the metal ratios of the deposits, and the compositions of the altered rocks, are consistent with the metals being leached mainly from this zone.

The hydrothermal fluids in the reaction zone are tapped by deeply penetrating, synvolcanic faults and discharged onto the seafloor or into permeable strata immediately below the seafloor. On nearing the seafloor, conductive cooling of the fluids, mixing with seawater, boiling, and reaction with the wall rocks cause the precipitation of sulfides and gangue minerals. Sulfide precipitation occurs initially in the subsurface, typically forming a network of sulfide veins (10–20% by volume) in intensely altered wall rock. Depending on the nature of the hydrothermal upflow and subseafloor permeability, the alteration pipe and stringer zone may extend tens to hundreds of meters below the massive sulfide deposits. Some stringer zones formed by focused, high-power hydrothermal discharge that forcibly brecciated the wall rock. Minerals typically deposited in the veins (mainly quartz, sulfides, and chlorite) continue up to the seafloor, where they are codeposited with the massive sulfides.

At the seafloor, sulfide deposition occurs in response to cooling, pH changes, and oxidation as the hydrothermal fluids mix with seawater. Mineral precipitation results in the accumulation of a sulfide mound around the vent. However, a number of different discharge scenarios are envisioned for different deposit types, depending on the temperatures and salinities of the ore-forming solutions (e.g., Sato, 1972). In some cases, the density of the hydrothermal fluid upon cooling is thought to have been greater than that of seawater, causing the solutions to flow into submarine depressions (e.g., **Figure 5**). In this case, precipitation of metals forms as a laterally extensive blanket rather than a sulfide mound (e.g., Solomon and Walshe, 1979; Solomon et al., 2004). Minerals that are only soluble at high temperature (e.g., chalcopyrite) are deposited close to the vent, producing a proximal Cu-rich ore, and minerals that are soluble at lower temperatures (e.g., sphalerite and galena) are deposited farther away, producing distal Zn–Pb ore. However, in most cases, the hydrothermal solution arriving at the seafloor is less dense than seawater and likely formed a buoyant hydrothermal plume. Minerals precipitated within the plume are commonly dispersed over a wide area by near-bottom and mid-depth currents.

Most large-tonnage VMS deposits formed at least partly or entirely by replacement of volcaniclastic rocks and sediments in high-permeability zones below the seafloor (e.g., Doyle and Allen, 2003; Gibson, 2005). The depth of emplacement below the seafloor ranges from a few tens to hundreds of meters, depending on the porosity and thickness of the clastic facies in the upper part of the volcanic pile, and the deposits are commonly stratabound or sheet-like in morphology. At depths of more than a few hundred meters below the seafloor, the clastic rocks are compacted, dewatered, and altered, and therefore less amenable to large-scale infiltration and replacement by hydrothermal fluids.

13.18.5 Chemical Evolution of the Hydrothermal Fluids

13.18.5.1 Fluid–Mineral Equilibria

VMS ore-forming fluids are acidic, reduced, 1–3 M chloride solutions in which metals were transported mainly as chloride complexes (**Table 3**). Before the discovery of black smokers, temperatures of the ore fluids were estimated from rare fluid inclusion data and sulfur isotope fractionation between sulfide

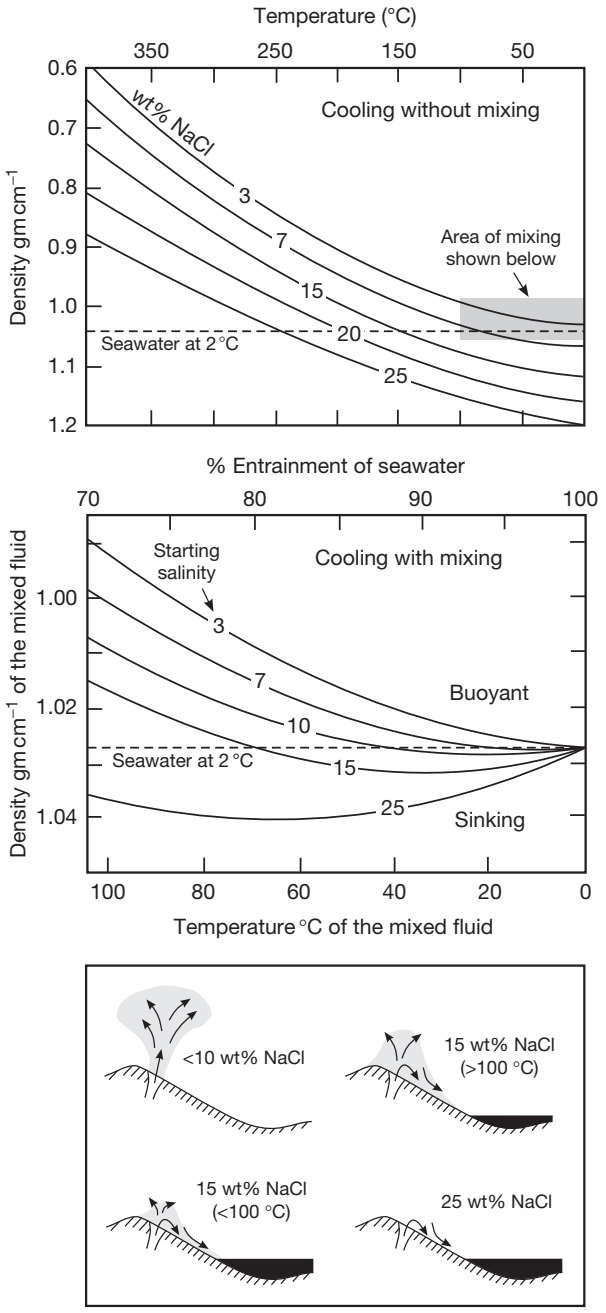

Figure 5 Densities of hydrothermal solutions with different salinities as a function of temperature at 200 bars (upper panel; data from Potter and Brown (1977)). Since most fluids are discharged at temperatures greater than 150 °C, bottom-seeking brines are rare, and only the most saline brines are more dense than seawater at the point of discharge. Mixing of 350 °C fluids having starting salinities of >10 wt% NaCl with cold seawater (middle panel) can result in fluids that are more dense than seawater and will descend and collect in brine pools (lower panel; adapted from Sato (1972); Turner and Campbell (1987). Nonlinear density effects during mixing may result in pulsed discharge, which in turn could give rise to the crude banding or bedding that is commonly observed in the Cu–Zn ores (e.g., **Figure 1**).

Table 3 Compositions of typical ore fluids responsible for VMS formation

	Ancient VMS	*Modern vents*	*Modern average*
pH	qtz–musc–kspar	2–5.8 (at 25 °C)	3.4 (at 25 °C)
NaCl (eq. wt %)	0.5–38	<1–8	3.5
H_2S (mmol)	py–po–mt	<1–40	7.3
CO_2 (mmol)	50–1000	<5–285	40
H_2 (mmol)	py–po–mt	<0.1–1.8	0.1–0.2
Metals (ppm)	7–450	10–1300	290

qtz–musc–kspar = pH range corresponding to quartz, muscovite, and K-feldspar equilibrium; py–po–mt = H_2S and H_2 range corresponding to pyrite, pyrrhotite, and magnetite equilibrium.

Sources: Hannington et al. (2005); Kajiwara (1973); Ohmoto et al. (1983); Pisutha-Arnond and Ohmoto (1983); Urabe (1974).

mineral pairs. pH values about 1 unit less than neutral (~5 at 250 °C) were determined from equilibrium with muscovite present in the stringer zones and estimated K^+ concentrations in the ore fluid (~0.1 M). Redox conditions were estimated from sulfide mineral equilibria, which also helped to constrain the likely sulfur content of the fluids (1–10 mmol). Metal concentrations were calculated from the solubilities of the ore minerals in solutions having salinities close to that of seawater. The physicochemical properties of the model fluids determined from these calculations are remarkably close to those of modern vent fluids (e.g., German and Von Damm, 2004). Comparisons with the chemistry of actively venting hydrothermal fluids from mid-ocean ridges have led to the present detailed understanding of the ore fluids, at least in basalt-hosted hydrothermal systems (Bowers et al., 1985, 1988; Janecky and Seyfried, 1984; Seyfried, 1987; Von Damm, 1988). In particular, the narrow range of fluid compositions is now recognized as reflecting strong chemical buffering by common greenschist facies alteration mineral assemblages (e.g., quartz–plagioclase–epidote–chlorite). Variations in fluid chemistry reflect different host-rock buffering (e.g., the role of sediments), phase separation, and possible contributions of magmatic brines and volatiles.

The behavior of seawater as a hydrothermal fluid was first established in experiments by Bischoff and Seyfried (1978) and Bischoff and Rosenbauer (1983). These experiments showed that many of the chemical characteristics of the ore fluids result simply from the heating of seawater. At ~150 °C, the concentrations of dissolved Ca^{2+} and SO_4^{2-} in heated seawater decrease sharply due to the precipitation of anhydrite, which has retrograde solubility, with SO_4^{2-} eventually reaching nearly zero concentration at temperatures above 400 °C. Some SO_4^{2-} is also reduced to hydrogen sulfide by reaction with ferrous Fe in the rock. Calcite similarly precipitates directly from seawater, due to its retrograde solubility, filling amygdules and other open spaces together with zeolites. At ~250 °C, magnesium begins to precipitate from seawater, incorporating Mg^{2+} in a brucite-like molecule ($Mg(OH)_2$) in minerals such as smectite, and generating acidity by the reaction, $Mg^{2+} + 2H_2O = Mg(OH)_2 + 2H^+$.

As seawater begins to react with the wall rocks in an intensifying hydrothermal system, sequential reactions and exchange of different elements take place at progressively higher temperatures along the flow path. Volcanic glass is quickly altered to clay minerals (mainly smectite) at temperatures up to about 100 °C (Alt et al., 1996; Gillis and Banerjee, 2000), causing alkali elements such as K^+, Rb^+, and Cs^+ to become fixed in the rock. Initially, this exchange is balanced by the leaching of Fe and Si from the glass. At >150 °C, the alkali elements that were previously fixed in the rocks at low temperatures are leached and replaced by Ca^{2+}, Mg^{2+}, and Na^+. Magnesium, in particular, is fixed first as Mg-rich smectite (<200 °C) and then as chlorite (>200 °C), which replace igneous plagioclase (eqn [1]). H^+ released during Mg fixation is partly consumed by the hydrolysis of the igneous minerals but also contributes to the overall acidity of the fluids. At about 250 °C, Na^+ is fixed as albite (also referred to as spilitization; eqn [2]):

$$4(Na,Si)_{0.5}(Ca,Al)_{0.5}AlSi_2O_8 + 15Mg^{2+} + 24H_2O \rightarrow 3Mg_5Al_2Si_3O_{10}(OH)_8 + SiO_2(aq) + 2Na^+ + 2Ca^{2+} + 24H^+$$

Albite–Anorthite in Basalt → Chlorite [1]

$$CaAl_2Si_2O_8 + 2Na^+ + 4SiO_2(aq) \rightarrow 2NaAlSi_3O_8 + Ca^{2+}$$

Anorthite → Albite [2]

$$3CaAl_2Si_2O_8 + Ca^{2+} + 2H_2O \rightarrow 2Ca_2Al_3Si_3O_{12}(OH) + 2H^+$$

Plagioclase → Epidote [3]

$$9CaAl_2Si_2O_8 + 1/2Fe_3O_4 + 3CaSO_4 + 11H_2 \rightarrow 6Ca_2Al_3Si_3O_{12}(OH) + 3/2FeS_2 + 8H_2O$$

Plagioclase + Anhydrite + Magnetite → Epidote + Pyrite [4]

In the highest temperature parts of the hydrothermal system (>350 °C), all Mg is lost from the hydrothermal fluid, and Ca fixation causes the formation of secondary plagioclase and epidote (eqn [3]; Saccocia et al., 1994; Seyfried and Ding, 1995), which releases even more H^+. At the same time, reaction of water with ferrous Fe-bearing minerals in the rock (e.g., olivine, pyroxene, and Fe sulfides) liberates metals and H_2 and results in major reduction of the fluids. Thus, the highest temperature fluids are in equilibrium with an assemblage of plagioclase–epidote–quartz–magnetite–anhydrite–pyrite, referred to as the PEQMAP buffer (eqn [4]).

Concentrations of H_2 and H_2S are fixed by pyrite–pyrrhotite–magnetite equilibrium and reflect reaction with immiscible sulfides and Fe-bearing olivine in the most reduced fluids and with a greenschist alteration mineral assemblage (PEQMAP buffer) in the most oxidised fluids (**Figure 6**). SiO_2 concentrations quickly rise to near quartz saturation (**Figure 7**). Downward-propagating fractures ensure a steady supply of fresh rock to buffer the fluids. These fractures commonly reach the top of the crystallizing subvolcanic intrusions and are filled with the minerals formed at the highest temperatures (e.g., quartz, epidote, and amphibole; Kelley et al., 1993; Gillis et al., 1993, 2001). In long-lived hydrothermal systems, a lack of continued fracturing and exposure of new crust to hydrothermal fluids may ultimately limit the supply of metals and other elements to the ore-forming fluids. The chloride concentration also determines the total concentration of metals that can be present in the fluid, as chlorocomplexes are the dominant metal-transporting agents. Chloride behaves conservatively, for the most part, and is by far the predominant anion in the hydrothermal fluids.

Comparisons with modern vent fluids show that the sum of reactions occurring along the path of hydrothermal circulation in basalt results in a fluid with an in situ pH of 4–5, salinity

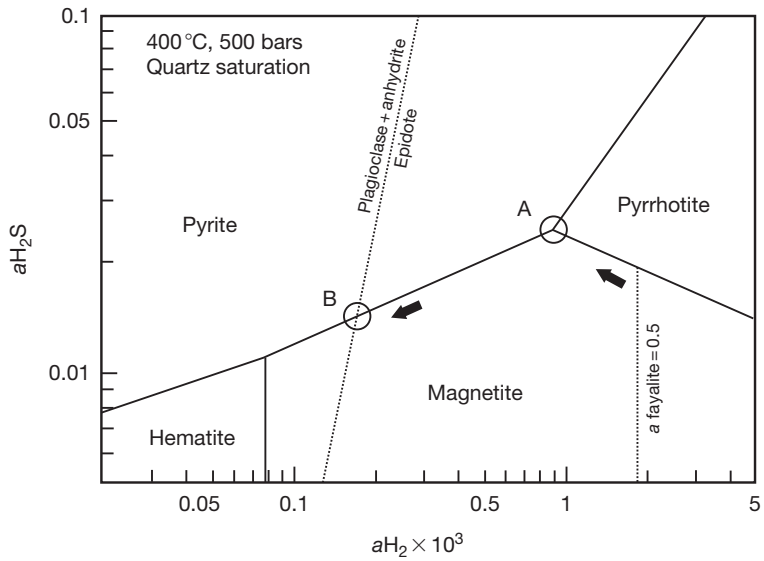

Figure 6 Redox evolution of ore-forming fluids in the reactions zones of VMS deposits. In the early stages of reaction (A), the fluids are close to equilibrium with pyrite, pyrrhotite, and magnetite in which H_2 and H_2S concentrations are buffered by the Fe–S–O assemblage. The final redox condition (B) is buffered by the assemblage plagioclase–epidote–quartz–magnetite–anhydrite–pyrite (PEQMAP buffer), resulting in a narrow range of H_2 and H_2S concentrations in the ore-forming fluids. Adapted from Seyfried WE Jr., Ding K, Berndt ME, and Chen X (1999) Experimental and theoretical controls on the composition of mid-ocean ridge hydrothermal fluids. *Reviews in Economic Geology* 8: 181–200.

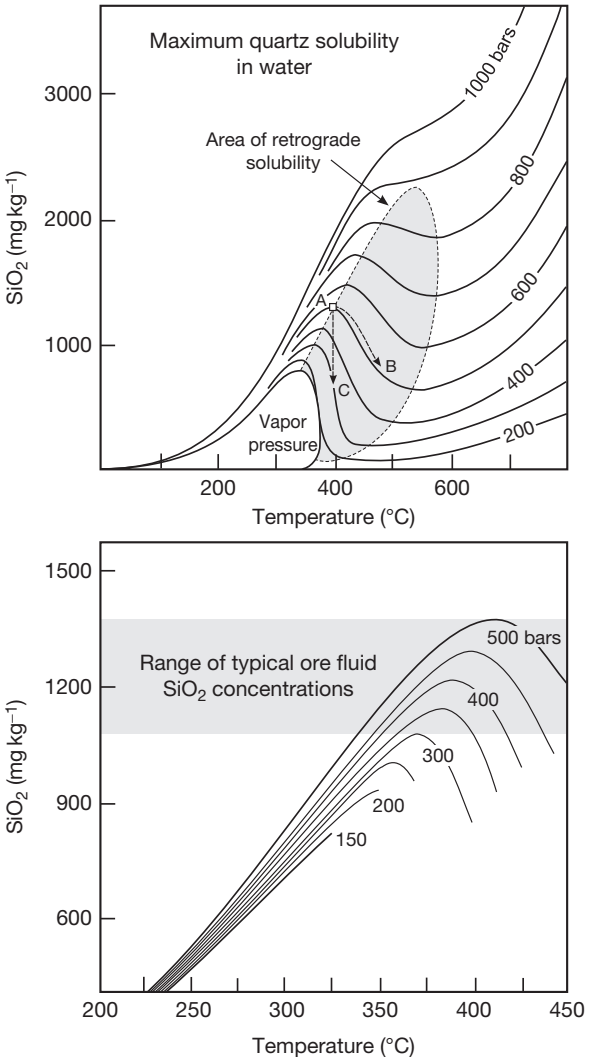

Figure 7 Solubilities of quartz in water at pressures from 200 to 1000 bars (upper panel, adapted from Fournier RO (1985) The behavior of silica in hydrothermal solution. *Reviews in Economic Geology* 2: 45–62) showing the field of retrograde solubility in which quartz precipitates at high temperatures during isobaric heating (path AB) or isothermal decompression (path AC). Solubility of quartz in seawater at the pressures and temperatures in the reaction zone (lower panel), indicating the range of typical ore-fluid concentrations of silica achievable at pressures equivalent to 300–500 bars (data from Von Damm et al., 1991).

of <1–8 eq. wt% NaCl (av. 3.5), CO_2 concentrations of <5–285 mmol (av. 40), H_2S concentrations of <0.1–41 mmol (av. 7.3), and H_2 concentrations of <0.1–1.8 mmol (av. 0.2) (cf. German and Von Damm, 2004). Fluids that have reacted mainly with felsic rocks have a wider range of compositions, with lower pH and higher aO_2. The few published experiments on seawater–rhyolite reactions (e.g., Hajash and Chandler, 1981) show a striking inverse correlation between the final pH of the solutions and the Si content of the rocks. pH is stabilized more quickly to lower values during reactions with felsic volcanic rocks, owing to a lack of Ca^{2+} leaching to balance the removal of Mg^{2+} from seawater. Thus, the dominant alteration assemblage in felsic volcanic rocks includes abundant K-rich clay minerals that form at pH values at least one unit more acid than muscovite–K-feldspar. However, recent seafloor observations suggest that a large part of the acidity in rhyolite-hosted hydrothermal systems may also be due to the presence of volcanic gases in the hydrothermal fluids (e.g., de Ronde et al., 2005).

13.18.5.2 Metal Concentrations

Metals and reduced sulfur that are leached from the rock reach maximum concentrations in the high-temperature reaction zone where they become major constituents of the hydrothermal fluids. Primary sulfides and ferromagnesian minerals in basalt are the major sources of Fe, Mn, Zn, and Cu; elements such as Pb and Ba are derived mainly from the dissolution of feldspars (e.g., Doe, 1994). Experiments involving the high-temperature reaction of seawater with basalt indicate that base metals are quantitatively leached at 375–385 °C and pressures of 300–500 bars, producing fluids that closely match black smokers in modern basalt-dominated systems (Seyfried and Ding, 1995; Seyfried et al., 1999). However, the metal concentrations are strongly dependent on the specific temperature, pH, chlorinity, and redox conditions in the reaction zone. Figure 8 shows the important role of chloro-complexing and especially temperature and redox in the mobility of Cu in the reaction zone. Temperatures in excess of ~350 °C are required for significant transport of Cu, and the most Cu is carried by fluids buffered at the highest oxidation states (e.g., hematite–magnetite–pyrite). In black smoker fluids, total concentrations of the transition metals average close to 300 ppm (~250 ppm Fe, 50 ppm Mn, 5–10 ppm Zn, 1–5 ppm Cu, and <0.1 ppm Pb) and range from <10 ppm in vapor-phase fluids to more than 1300 ppm in some brines (German and Von Damm, 2004). These concentrations are lower than expected for mineral solubilities in the reaction zone (e.g., Figure 8) and suggest that metal deposition occurred below the seafloor or that the fluids in the reaction zone were undersaturated with metals. At the much lower temperatures of the discharge zone, most ore solutions were likely close to saturation with respect to the major ore minerals, thus explaining the strong metal zonation in the deposits (see below).

The concentrations of some trace elements, such as Co, Se, Mo, Cd, As, Sb, Ag, and Au, also have been determined in vent fluids (Butterfield et al., 1994; Seyfried et al., 2003; Trefry et al., 1994; Von Damm, 1990). Although these data are scarce, different elements usually display consistent enrichments and depletions as a function of temperature (e.g., Auclair et al., 1987; Hannington et al., 1991). Co, Se, and Mo show a strong positive temperature–concentration relationship in the fluids and are enriched in high-temperature Cu-rich sulfides. Other elements such as Cd, Pb, As, Sb, and Ag are enriched in lower temperature fluids and concentrated in Zn-rich sulfides. Considerable attention has been paid to the precious metal concentrations of the deposits, as gold and silver are notably high in some cases (Hannington et al., 1999b, and references therein; Huston and Large, 1989). Analyses of black smoker fluids and their quenched products indicate gold concentrations in the range of 0.05–0.2 $\mu g\,kg^{-1}$. However, recent data from seawater-dominated hydrothermal fluids in the

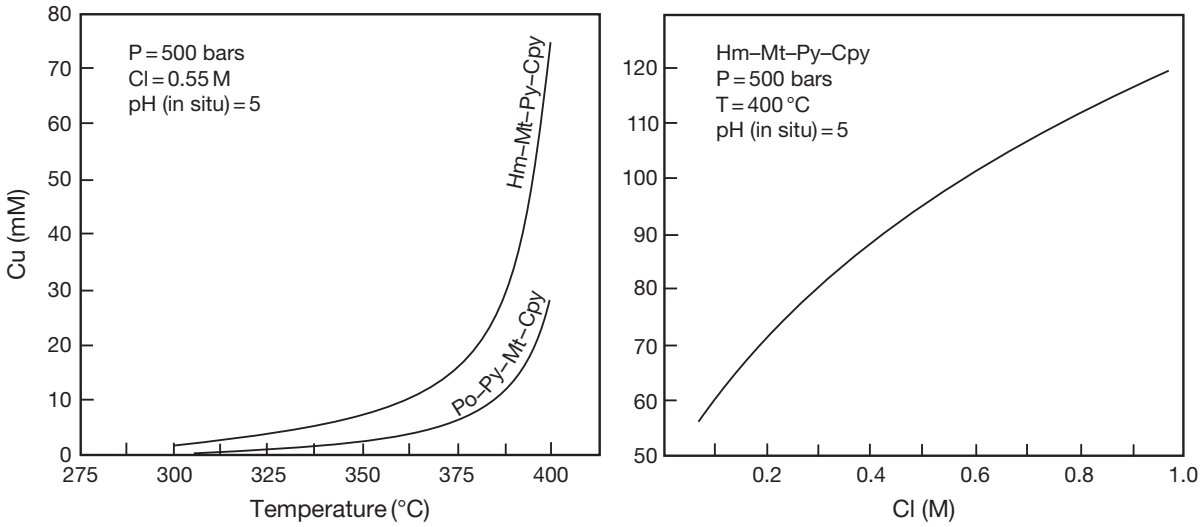

Figure 8 Solubility of chalcopyrite for two different redox buffers, pyrrhotite–pyrite–magnetite and hematite–magnetite–pyrite, as a function of temperature (left panel) and chloride concentration (right panel) under conditions typical of the reactions zones of VMS deposits. Adapted from Seyfried WE Jr. and Ding K (1995) Phase equilibria in subseafloor hydrothermal systems: A review of the role of redox, temperature, pH, and dissolved Cl on the chemistry of hot spring fluids at mid-ocean ridges. In: Humphris SE, Zierenberg RA, Mullineaux LS, and Thomson RE (eds.) *Seafloor Hydrothermal Systems: Physical, Chemical, Biological, and Geological Interactions, Geophysical Monograph Series*, vol. 91, pp. 248–272. Washington, DC: American Geophysical Union.

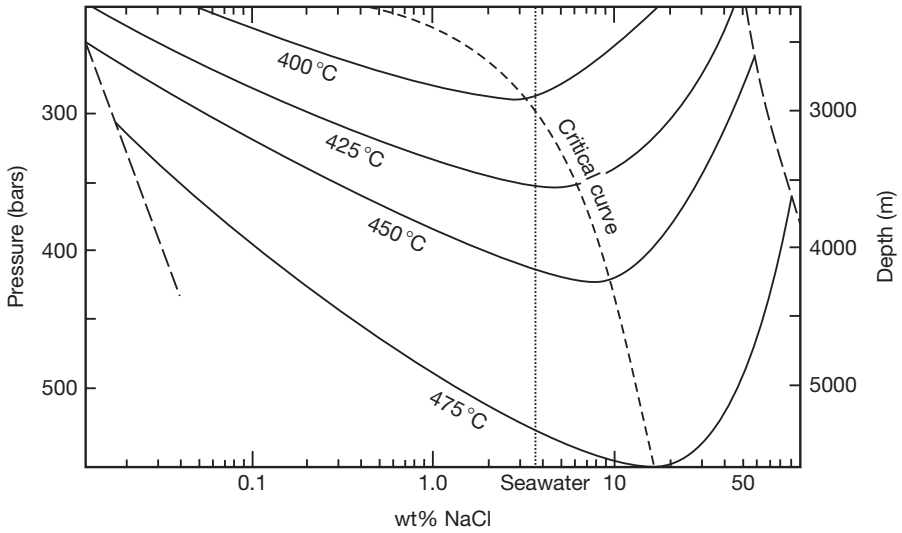

Figure 9 Phase diagram for the NaCl–H_2O system. Fluids intersecting the critical curve at temperatures higher than the critical temperature (407 °C) separate into a conjugate pair of high- and low-salinity fluids with compositions indicated by the respective solvus. Adapted from Scott SD (1997) Submarine hydrothermal systems. In: Barnes HL (ed.) *Geochemistry of Hydrothermal Ore Deposits*, 3rd edn., pp. 797–875. New York: Wiley; and data in Bischoff and Pitzer, 1989.

Reykjanes geothermal system of Iceland suggest that these may be minimum values (Hardardóttir et al., 2009).

13.18.5.3 Role of Phase Separation

In the reaction zone, some fluids reach temperatures and pressures higher than the critical point of seawater; on cooling and/or depressurization to the critical curve, a small amount of high-salinity brine condenses from the bulk fluid (Figure 9). This behavior was first examined in detail by the experiments of Bischoff and Rosenbauer (1984) and Bischoff and Pitzer (1985). The effects of supercritical phase separation also have been documented at seafloor vents (Butterfield and Massoth, 1994; Butterfield et al., 2003), and supercritical fluids have recently been sampled in the deepest hydrothermal systems on the mid-ocean ridges (e.g., Koschinsky et al., 2008). During phase separation, dissolved gases such as CO_2, H_2, and H_2S partition strongly into the less dense phase together with

neutral species such as HCl and H_4SiO_4; chloride is partitioned into the more dense liquid. The majority of monovalent cations, such as Na^+, are not fractionated relative to chloride, but divalent cations such as Ca^{2+} and the transition metals become highly concentrated in the brine phase. Solubilities of metals as aqueous chloride complexes in the brine are several orders of magnitude greater than in fluids of seawater composition (Bischoff and Rosenbauer, 1987). Foustoukos and Seyfried (2007) also predicted that some metals would partition into the less dense liquid as aqueous sulfur complexes (e.g., As > Sb > Au > Fe > Cu > Zn > Ag), resulting in the transport of these elements in the vapor-rich phase. The high density of the brine phase raises the possibility that these liquids may become physically separated from the less dense vapor-rich phase (e.g., in high-temperature brine reservoirs at depth) and thereby have a unique discharge history (Bischoff and Rosenbauer, 1989; Coumou et al., 2009; Fontaine and Wilcock, 2006). This scenario is supported by observations of chemically complex, hypersaline fluids, including both NaCl- and $CaCl_2$-immiscible liquids and high-density CO_2-rich liquids in fluid inclusions in veins from the reaction zone, locally having salinities of up to 50 eq. wt% NaCl (Kelley and Früh-Green, 2001). Small quantities of these liquids may become incorporated in the high-temperature upflow with important implications for metal transport to the seafloor.

Paleogeographic evidence for some VMS deposits indicates water depths as shallow as 300–500 m, with some deposits having formed in volcanic successions that were at least partly emergent (Franklin et al., 2005; Gibson, 2005). Fluids in these hydrothermal systems undoubtedly boiled. At typical water depths of VMS formation (e.g., 2500–3000 m), most ore fluids at the point of discharge would be well below the two-phase (liquid + vapor) curve for seawater. However, at shallower depths, fluids rising to the seafloor may intersect the two-phase boundary for seawater at pressures and temperatures well below the critical point (**Figure 10**). At 1500 m water depth, the near-vertical adiabats of most fluids at 350 °C will intersect the two-phase boundary about 100 m below the seafloor, and the fluid will boil continuously from that depth as it rises to the seafloor. At these low pressures, the density difference between the vapor and liquid is much greater than in the reaction zone, resulting in the rapid separation of a low-salinity, gas-rich phase. Cooling of the hydrothermal fluids as a result of boiling will determine where ore deposition commences. Vertically extensive vein mineralization in some VMS deposits may be an indication of strong cooling that was coincident with subseafloor boiling. The boiling depth increases dramatically for gas-rich fluids, and a large magmatic volatile component may cause a deeper boiling zone, possibly resulting in no massive sulfide formation on the seafloor. Thus, there are important physical limitations to the water depth at which high-temperature sulfides can form at the seafloor if the pressure is insufficient to prevent boiling. It is unlikely that a Cu-rich massive sulfide deposit could develop at water depths of less than 500 m, corresponding to a boiling temperature of <265 °C, unless the composition of the hydrothermal fluids was very different from that of seawater (e.g., a high-salinity brine). The cooling that accompanies decompression and boiling in shallow water will cause metals such as Cu, which is

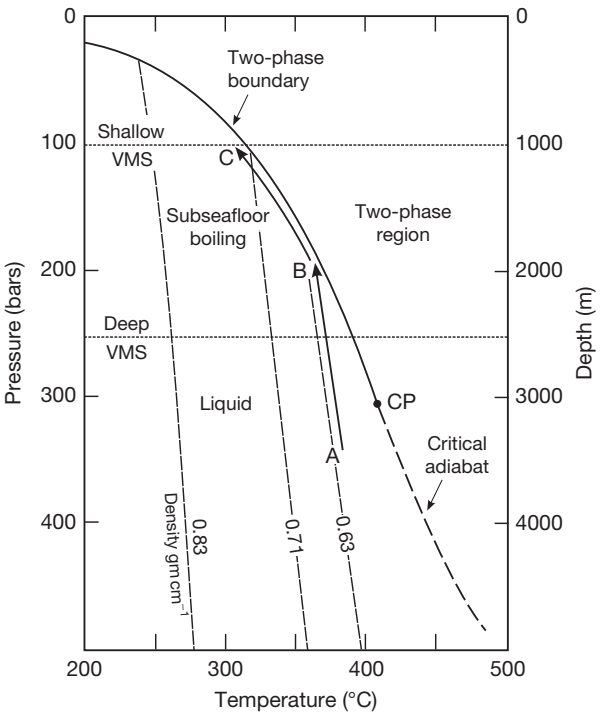

Figure 10 Two-phase curve for seawater (solid line) separating the liquid stability field from the liquid + vapor field, and indicating the location of the critical point of seawater (CP) at 407 °C and 298 bar. Diagonal lines are the adiabats for fluids of different density; maximum fluid flow occurs at temperatures and pressures close to the critical point. Fluids rising to the seafloor at great depth (path AB) will remain in the liquid field; fluids that interact the boiling curve below a shallow seafloor (path BC) will boil below the seafloor before discharging at shallow VMS. Adapted from German CR and Von Damm KL (**Chapter 8.7**).

most effectively transported at high temperature, to be deposited in the subseafloor boiling zone. Metals that are transported at lower temperatures (e.g., Au, Ag, As, Sb, Hg, Tl, Pb, and Zn) tend to be concentrated above the boiling zones and are notably enriched in deposits that formed in shallow water (Hannington et al., 1999b).

13.18.5.4 Redox Controls on Ore Deposition

Differences in pH and oxidation state of the fluids, which have a major impact on the mineralogy of the deposits, reflect a combination of the strong chemical buffering in the reaction zone and different mixing–cooling histories. Precipitation of sulfides at the seafloor is mainly due to cooling and pH increase. However, because of the high concentrations of reduced components, such as ferrous iron, H_2, and H_2S, the fluids do not deviate significantly from their original redox buffer as they rise to the seafloor (**Figure 11**). Deposits that are formed by fluids that have equilibrated mainly with mafic volcanic rocks are buffered at intermediate aO_2 values and produce both pyrite and pyrrhotite. Fluids that have equilibrated mainly with felsic volcanic rocks tend to be more oxidized and have a lower redox-buffering capacity because of the lower abundance of FeO-bearing minerals in the rock. Thus, pyrite is the dominant mineral in felsic-hosted deposits;

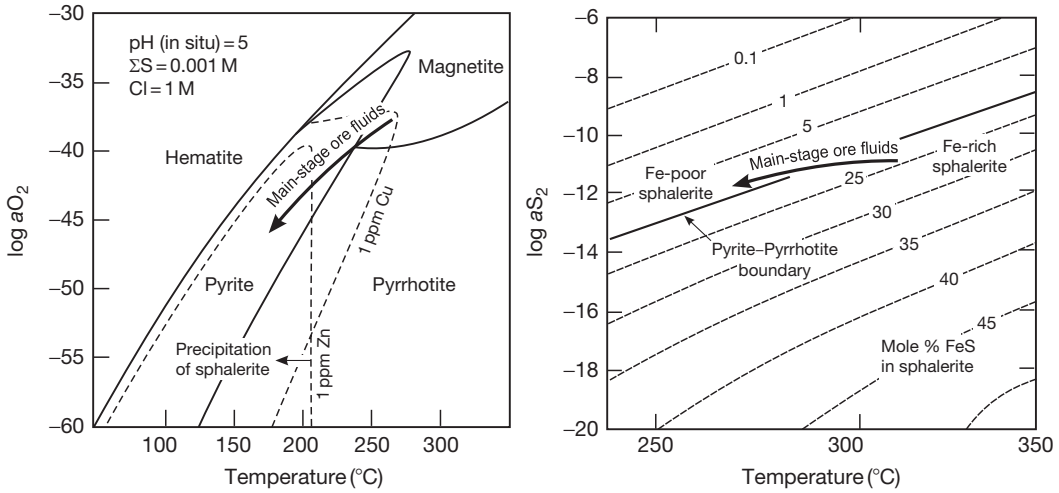

Figure 11 aO_2–temperature diagram (left panel) at pH (in situ) = 5 and total sulfur concentration of 0.001 M showing the stability fields of the principal Fe–S–O minerals. Main-stage ore fluids of most VMS deposits are buffered by reaction with volcanic rocks at high temperatures close to pyrite–pyrrhotite–magnetite equilibrium with aO_2 decreasing as the fluids cool. Solubilities of chalcopyrite and sphalerite (1 ppm each) show that fluids buffered initially by pyrite–pyrrhotite–magnetite will first precipitate chalcopyrite and then sphalerite on cooling (adapted from Large RR (1977) Chemical evolution and zonation of massive sulfide deposits in volcanic terrains. *Economic Geology* 72: 549–572). The right panel shows that the composition of sphalerite generally decreases with decreasing temperature under the same conditions (adapted from Barton PB Jr and Skinner BJ (1979) Sulfide mineral stabilities. In: Barnes HL (ed.) *Geochemistry of Hydrothermal Ore Deposits*, 2nd edn., pp. 278–403. New York: Wiley).

pyrrhotite is less common. Fluids that have reacted extensively with organic-rich sediments or ultramafic rocks may have significantly more reduced compositions, which gives rise to a class of deposits that are mineralogically quite different from those in less mafic or felsic-dominated volcanic assemblages. Reactions with sediments generally result in higher pH, and organic matter in the sediments buffers the fluids to very low aO_2. Pyrrhotite is the dominant Fe sulfide phase, and other minerals that typically formed at low aO_2 are commonly present (e.g., Fe-rich sphalerite, arsenopyrite, and loellingite). Calcite, dolomite, manganiferous carbonate, Mg silicates (e.g., talc), and even hydrocarbons, are also important constituents of the hydrothermal precipitates in sediment-hosted VMS.

Mixing of sulfur-rich magmatic volatiles with the ore fluids may lead to highly acidic, oxidizing conditions, with the formation of distinctive high-sulfidation mineral assemblages (e.g., containing enargite, luzonite, tennantite, covellite, native sulfur, and alunite; Hannington et al., 1999b; Sillitoe et al., 1996). The compositions of several common sulfide minerals are very sensitive to the redox conditions. In particular, the compositions of sphalerite, pyrrhotite, and arsenopyrite have been calibrated experimentally against temperature, aO_2, and aS_2 (e.g., Figure 11) and offer a means by which to monitor changes in these parameters during mineralization.

13.18.6 Metal Zoning and Trace Element Geochemistry

13.18.6.1 Metal Zoning

Most deposits are compositionally zoned according to the solubilities of the different ore minerals, with Cu- and Fe-rich sulfides being most abundant in the interiors and in the underlying stockwork zones of the deposits, and Zn- and Pb-rich sulfides deposited at the outer margins. Solubility contours for chalcopyrite and sphalerite, superimposed on the Fe–S–O system (Figure 11), show that the zoning of most VMS deposits can be accounted for by a cooling path that sequentially crosses the stability fields of magnetite, pyrrhotite, and pyrite, first precipitating chalcopyrite and then sphalerite. Thus, the high-temperature Cu-rich stringer zones of many deposits are dominated by pyrrhotite ± magnetite, whereas lower temperature Zn-rich massive sulfide zones are dominated by pyrite. If the compositions of the hydrothermal fluids are known, a thermal profile of the different ore zones can be confidently reconstructed based on calculated saturation temperatures of the ore minerals. In the model depicted in Figure 12, most of the chalcopyrite is deposited at temperatures between 350 and 250 °C, but the fluids do not become saturated with sphalerite until about 250 °C.

The resulting Cu–Zn zonation (Cu below Zn) is so consistent that it has long been used in deformed terranes as an indicator of stratigraphic facing direction (e.g., Figure 13; Sangster, 1972; Sangster and Scott, 1976). The same zoning is seen at a variety of scales. In modern black smoker chimneys, high-temperature fluid conduits are commonly lined by chalcopyrite, and the cooler outer rims are made up of the minerals deposited at lower temperature (sphalerite, pyrite, and marcasite). In most deposits, the high-temperature hydrothermal fluids cooled well below the saturation temperature for chalcopyrite before discharging at the seafloor, resulting in the strong vertical zonation of Cu and Zn in the sulfide mounds. At a much larger scale, deposits that formed close to their vent commonly have a high Cu/Cu + Zn ratio, whereas deposits that formed at lower temperatures, distal to the discharge sites, have lower Cu/Cu + Zn ratios (Figure 13). The degree of separation of minerals having different

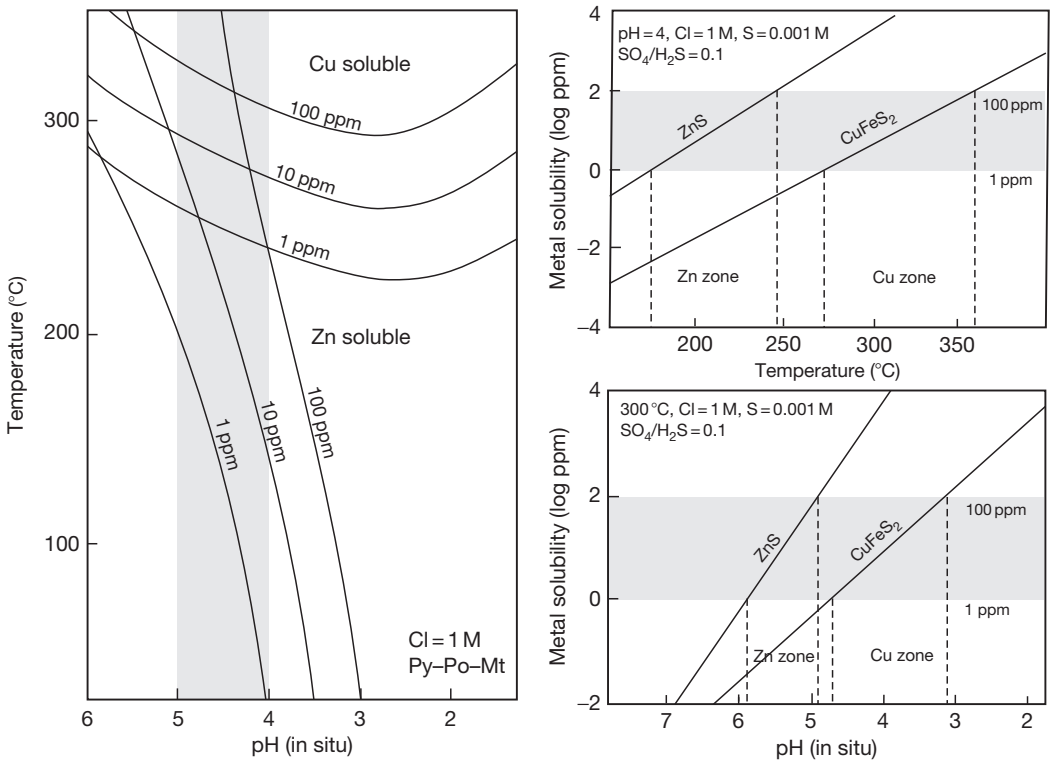

Figure 12 Solubilities of chalcopyrite and sphalerite in fluids buffered by pyrite–pyrrhotite–magnetite as a function of pH (in situ) and temperature (left panel). Solubilities of chalcopyrite range from 1 to 100 ppm Cu in fluids at 250–350 °C; solubilities of sphalerite range from 1 to 100 ppm Zn at temperatures up to 250 °C. During mixing and cooling, chalcopyrite and sphalerite are deposited in sequence according to their respective solubilities as a function of decreasing temperature and increasing pH (right panels). A typical ore-forming fluid will become saturated with respect to chalcopyrite at high temperatures and precipitate a Cu-rich zone; the same fluid at lower temperatures will eventually become saturated with respect to sphalerite and precipitate a Zn-rich zone. Adapted from Large RR (1992) Australian volcanic-hosted massive sulfide deposits: Features, styles, and genetic models. *Economic Geology* 87: 549–572.

solubilities is strongly affected by the mixing–cooling history of the ore solutions. Sphalerite precipitation is mostly driven by an increase in pH (e.g., Bourcier and Barnes, 1987). During mixing of hydrothermal fluids with seawater, this leads to rapid codeposition of chalcopyrite and sphalerite (**Figure 12**). However, during conductive cooling, pH changes are limited and aH^+ may even increase as a result of the production of acid during sulfide deposition. In this case, the lower pH of the fluids inhibits the precipitation of sphalerite, resulting in more effective separation of Cu and Zn. The predominance of Zn-rich, pyrite–sphalerite ores in some large-tonnage deposits implies that most of the ore was deposited at relatively low temperatures (e.g., <300 °C) and that Cu either was not mobilized by the hydrothermal fluids or was deposited below the seafloor. Because Zn and Pb are easily leached from volcanic rocks and effectively transported at low temperatures, a long-lived, low-intensity hydrothermal system could account for most of the metal in large Zn-rich deposits, whereas smaller, Cu-rich deposits must have formed at much higher temperatures (e.g., Large, 1992).

One assumption in these models is that all of the minerals were precipitated from the same fluid in a uniform physicochemical gradient. However, the deposits can be paragenetically complex, with multiple replacement or overprinting events arising from highly variable thermal histories. Petrographic examination commonly reveals complex intergrowths and replacement textures that reflect the dynamic and locally chaotic environment of sulfide precipitation. Much of the ore deposition in a thermally intensifying system occurs by infilling and replacement of preexisting sulfides, where early fine-grained minerals are overgrown by coarser grains, significantly reducing the porosity of the massive sulfides. Ores that have been affected by this process show signs of extensive hydrothermal recrystallization and annealing. At the smallest scale, this is seen as a common texture in sphalerite where higher temperature Cu-rich fluids have introduced fine intergrowths or disseminations of chalcopyrite (so-called chalcopyrite disease; Barton and Bethke, 1987). At a larger scale, secondary mineralogical zoning can develop as previously deposited minerals are exposed to a succession of later higher- or lower-temperature fluids. This process of hydrothermal reworking or 'zone-refining' originally described by Barton (1978) and adapted to the Kuroko deposits by Eldridge et al. (1983) involves the continuous dissolution and reprecipitation of earlier formed minerals by the flow of high-temperature fluids through the deposit. Over time, this process can strip Zn from the interior of a deposit and reprecipitate it at the cooler outer zones, leaving Cu behind; 'over-refining' can destroy a potentially economic deposit, leaving only barren pyrite (e.g., Hannington et al., 1998).

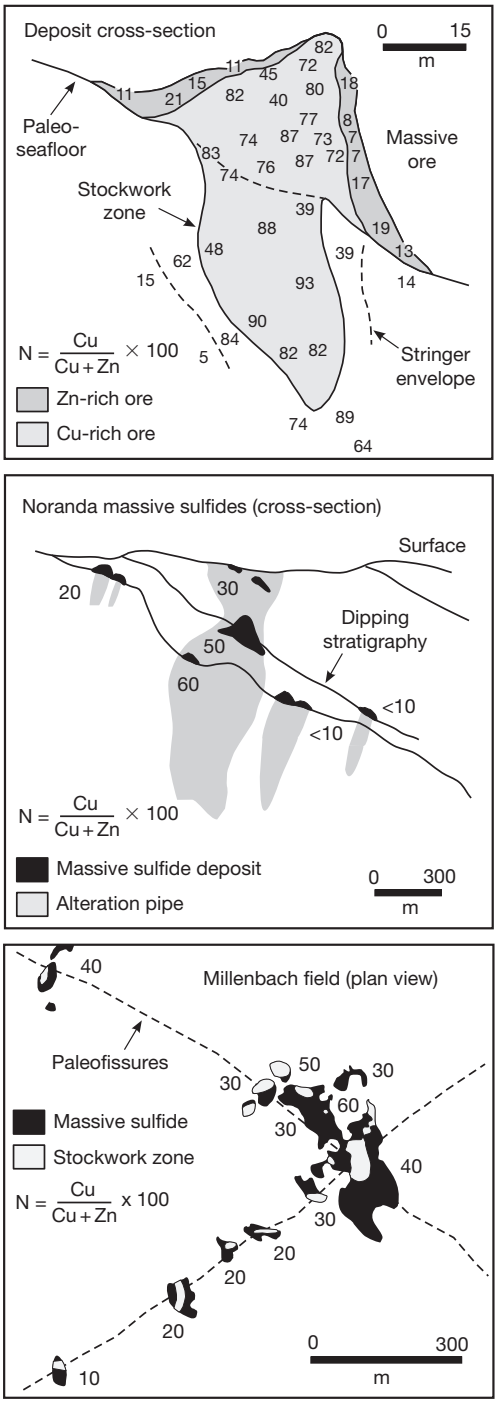

Figure 13 Schematic illustrations of metal zoning at different scales in a typical VMS district (Noranda, Quebec). The upper panel shows Cu–Zn zoning (in terms of Cu/Cu + Zn ratios) in a small massive sulfide deposit with a Cu-rich core and Zn-rich outer margin. The middle panel shows a decrease in Cu/Cu + Zn with stratigraphic height in a stacked ore system. The lower panel shows higher Cu/Cu + Zn ratios in deposits at the center of a field and lower ratios in deposits farther from the main upflow zone. Adapted from Knuckey MJ, Comba CDA, and Riverin G (1982) Structure, metal zoning, and alteration at the Millenbach deposit, Noranda, Quebec. In: Hutchinson RW, Spence CD, and Franklin JM (eds.) *Precambrian Sulfide Deposits*, *Geological Association of Canada Special Paper* 25, pp. 255–296. St. John's, NL: Geological Association of Canada.

Table 4 Concentration ranges of selected trace elements in VMS deposits

Concentrations	*Trace elements*
To 10 000 ppm	As, Sb, Cd
To 1000 ppm	Co, Sn, Se
To 500 ppm	Ni, Mo, Bi, In, Te
To 100 ppm	Hg, Tl, W, Ge, Ga

13.18.6.2 Trace Element Geochemistry

As noted above, sulfide mineral assemblages that formed at different temperatures almost always have consistent enrichments in different trace metals (Table 4). Two main trace element associations are commonly recognized: a low-temperature, polymetallic assemblage of Zn, Pb, Ag, Cd, Sn, Sb, As, Hg, ±Tl, ±W, and a higher temperature suite of Cu, Co, Bi, Se, In, ±Ni, ±Mo. Because the solubilities of chalcopyrite and sphalerite as $CuCl_2$ and $ZnCl_2$ are well known, strong coenrichments of trace elements together with Cu or Zn provide a clear indication of their behavior in the hydrothermal fluids, even when the solubilities of their host ore minerals have not been determined experimentally. The behavior of the trace elements is dictated by the stability of various aqueous complexes as reviewed by Wood et al. (1987), Seward and Barnes (1997), Wood and Samson (1998), and Seward et al. (**Chapter 13.2**) and summarized for VMS systems below. Some elements, such as Ag and Sn, may be enriched in both high-temperature (Cu-rich) and low-temperature (Zn-rich) mineral assemblages as different mineral phases (e.g., Ag-rich chalcopyrite and Ag-rich tetrahedrite; Cu–Sn-sulfides and cassiterite). The distribution of other trace elements is more closely linked to mineral-chemical controls, such as the solid solution of Cd in sphalerite.

Gold and silver enrichment is commonly associated with high concentrations of Zn, As, Sb, and Pb, and locally with high Hg and Tl. The latter form stable aqueous complexes under conditions similar to those required for the transport of gold as $Au(HS)_2^-$. However, other deposits exhibit a strong Cu–Au association that is attributed to higher temperature gold-chloride complexing ($AuCl_2^-$). Gold is most readily transported in VMS-forming solutions at near-neutral conditions and high aO_2; strongly reduced fluids are well outside the range of maximum solubility of gold as either $Au(HS)_2^-$ or $AuCl_2^-$. The latter type of fluid has been suggested to explain the low gold contents of sediment-hosted massive sulfide deposits, which are typically dominated by reduced, pyrrhotite-rich mineral assemblages (Hannington and Scott, 1989; Huston and Large, 1989).

Other elements that form stable aqueous sulfur complexes, such as $Sb_2S_2(OH)_2$ and $HSb_2S_4^-$, also tend to be incorporated in sulfides at lower temperatures. Ag(I) chloride complexes ($AgCl_2^-$) dominate the transport of Ag in most hydrothermal fluids at temperatures >200 °C and pH < 5, but $Ag(HS)_2^-$ may be important at lower temperatures and higher pH. Huston et al. (1995b) noted that low temperature, oxidizing conditions favored the partitioning of Ag into sulfosalts such as tetrahedrite, whereas higher temperature, reduced conditions favored partitioning into Ag-rich chalcopyrite. Pb(II) chloride complexes ($PbCl_2$) are predominant at low temperatures,

although $Pb(HS)_2$ may also be important in near-neutral, sulfur-rich fluids at temperatures below about 200 °C.

Arsenic occurs both in common sulfosalts in Zn-rich assemblages and in arsenopyrite, Cu–As sulfides, and Co–As-sulfides in higher temperature, Cu-rich assemblages. Arsenious acid complexes (e.g., H_3AsO_3) account for most of the arsenic in solution at high temperatures (down to about 200 °C), but thio complexes of arsenic (e.g., $HAsS_2$) are likely important at lower temperatures. At low aO_2, the stability field for arsenopyrite overlaps that of pyrrhotite, and the close association of arsenopyrite with pyrrhotite in many deposits is consistent with moderately to strongly reduced ore fluids. In other VMS deposits, the association of arsenopyrite with pyrite implies an expanded field of stability for arsenopyrite, possibly caused by higher concentrations of As in the ore-forming fluids.

Deposits with high Sn commonly have a low-aO_2 mineral assemblage, for example, containing abundant pyrrhotite, arsenopyrite, high-Fe sphalerite, Fe-rich chlorite, or siderite. The presence of Cu–Sn sulfides in these ores also has been interpreted as evidence of Sn being introduced by high-temperature Cu-rich fluids of probable magmatic origin (e.g., Hannington et al., 1999a; Huston et al., 2010b). In contrast, cassiterite can be quite soluble as $SnCl_2$ in solutions of moderate salinity at low temperatures down to at least 200 °C. This is consistent with the precipitation of cassiterite at low temperatures in a number of other deposit types, including chemical sediments associated with VMS (e.g., Lehman, 1991).

A strong correlation between Cu and In exists in many deposits. Indium forms stable chloride complexes only at high temperatures, low pH, and high salinity (e.g., $InCl_3$), which explains the association with Cu-rich ores. Similar enrichments are evident at hydrothermal vents on the modern seafloor, where In is deposited with chalcopyrite at ~350 °C in the cores of some black smoker chimneys (e.g., Fouquet et al., 1993). Roquesite ($CuInS_2$) is the predominant In-bearing phase, commonly occurring as trace inclusions in sphalerite, similar to 'chalcopyrite disease.' Typically, the highest concentrations of In occur along replacement fronts between massive chalcopyrite and massive sphalerite ore, indicating that In was most likely introduced at high temperatures together with Cu. However, like Ag and Sn, In may be enriched in both high-temperature (Cu-rich) and low-temperature (Zn-rich) ores in different mineral phases.

Enrichments of Co, Bi, Ni, and Mo are also common in massive chalcopyrite and chalcopyrite stringer ores of many VMS deposits. Co and Mo are transported mainly as chlorocomplexes (e.g., $CoCl_4^{2-}$) and oxyacids (e.g., H_2MoO_4) that are most stable at high temperatures. Bismuth is transported mainly as oxyanions (e.g., $Bi(OH)^{2+}$ and $Bi(OH)_3$), although Bi-chloride complexes are also known, and these similarly have maximum stabilities at high temperatures. One of the most common Bi minerals in VMS ores, bismuthinite, is sparingly soluble except at temperatures greater than 350 °C and salinities of at least 5 m NaCl (cf. Wood et al., 1987), consistent with its occurrence only in Cu-rich ores. Ni occurs most commonly as a trace constituent of pyrite, but is also found as cobaltite or Co-pentlandite in massive chalcopyrite and chalcopyrite stringer ores, especially in deposits with mafic or ultramafic footwalls (see below).

Selenium also shows a strong correlation with Cu in most deposits. Selenium is carried in the fluid phase as a volatile species similar to H_2S, but because of the strong pH and temperature dependence of the dissociation constant for H_2Se, it is partitioned as a trace element into the highest temperature sulfide minerals. Selenium mainly substitutes for sulfur in the principal Cu and Fe sulfides, although discrete selenide minerals can account for a significant proportion of the Se in some Cu-rich ores (e.g., Hannington et al., 1999a; Layton-Matthews et al., 2008; **Table 2**). Huston et al. (1995a) also argued that high H_2Se/H_2S ratios in some ore-forming fluids are most likely caused by a significant magmatic input. Tellurium occurs in trace amounts as base- and precious metal tellurides in many VMS ores; however, Te is far less abundant than Se overall.

Zone refining and boiling may also control the distribution of trace elements in some deposits, such as the common enrichment of Au and Ag at the tops of some deposits and their overall depletion in the interiors. Other elements of the so-called epithermal suite (e.g., As, Sb, Hg, and Tl) are highly enriched in deposits that formed from boiling hydrothermal fluids and locally form a distinctive halo in the hanging wall above some deposits (e.g., Hannington et al., 1999a,b). Concentrations of up to several tens of ppm Hg are common in massive sphalerite, but the Cu-rich ores of most deposits rarely contain more than a few hundred ppb. The highest concentrations of Tl typically occur in massive pyrite or pyrite stringer mineralization, but Tl is also enriched in clay minerals surrounding the deposits (e.g., Large et al., 2001). The distribution of some of these elements may be controlled by metal transport in the vapor phase.

Manganese is present at high concentrations in most reduced fluids in VMS-forming systems but is rarely abundant in the ores. It does not form a stable sulfide mineral under most conditions of ore formation, although alabandite (MnS) is present in some metamorphosed deposits. Instead, Mn is lost to distal hydrothermal facies, for example, chemical sediments, or is contained within gangue minerals (e.g., manganiferous siderite or garnet; see below).

13.18.6.3 Sources of Trace Metals

The concentrations of most trace elements in the ores, especially those that are mobilized at relatively low temperatures, are remarkably sensitive to source rock concentrations. Whereas most VMS ore solutions would have been close to saturation with respect to the major ore minerals, they were likely highly undersaturated in trace metals, and the ability to leach these elements from the rock should not have been a limiting factor for their abundance in the deposit. Thus, although volcanic rocks such as basalt generally have very uniform concentrations of transition metals, small variations are clearly reflected in the associated VMS deposits. For example, VMS deposits with mafic-dominated or mafic–ultramafic footwalls are commonly enriched in Co and Ni. It has been shown that Co and Ni released from olivine and other ferromagnesian minerals during the early stages of serpentinization react with reduced sulfur in the hydrothermal fluids to produce trace amounts of millerite (NiS) and pentlandite $(Fe,Ni)_9S_8$ in the altered rock (Alt and Shanks, 2003); these metals are leached by later hydrothermal fluids and reprecipitated in the massive sulfide deposits. Felsic volcanic rocks typical of subduction-related volcanic arc environments, especially in areas of continental basement, are enriched by Pb, As, Sb, Ag,

and Sn, and the sulfide deposits hosted in these rocks have correspondingly higher average concentrations of these elements than deposits in mafic volcanic-dominated settings (Shikazono, 2003; Stanton, 1994). Enrichment in trace elements such as Hg may reflect preconcentration in organic matter or diagenetic sulfides in sediments within the volcanic pile (e.g., Barnes and Seward, 1997).

In many deposits, significant coenrichment of elements such as Cu, Bi, Se, and In has been argued as evidence for direct contributions of metals from magmatic fluids (e.g., Large, 1992). The basis for suggesting that these elements may be magmatically derived is their common association in porphyry Cu deposits as well as experimental evidence for their strong partitioning into aqueous fluids during crystallization of felsic magmas (e.g., Candela and Piccoli, 2005). In other deposits, high concentrations of elements such as Sn, W, and F, together with high $\delta^{18}O$ values for the ore fluids, offer the most convincing evidence for a direct contribution to the hydrothermal fluids from a felsic magmatic source (Huston, 1999; Huston et al., 2010a).

13.18.7 Nonsulfide Gangue Minerals

The dominant gangue minerals in VMS ores are quartz, chlorite, muscovite, carbonates, and sulfates (mainly gypsum and barite). The same minerals form the dominant alteration in host rocks affected by the ore fluids (see below). Minor albite, epidote, amphibole, and tourmaline may also be present in the ores. Metamorphic minerals derived from the ore-related gangue are common in deposits that have attained upper greenschist to amphibolite grades (e.g., manganiferous garnet, Zn-rich staurolite, and the Zn spinel, gahnite; see **Chapter 13.7**). Importantly, the sulfate minerals are rare or absent in most Archean deposits, owing to the lack of sulfate in Archean deep seawater.

Although quartz is saturated in most VMS-forming fluids, its precipitation is inhibited due to kinetic barriers at the low pH of the fluids (Fournier, 1985). Amorphous silica probably was the main form of SiO_2 deposited at the seafloor, precipitating only after the fluids cooled well below amorphous silica saturation (**Figure 14**). Thus, much of the quartz now preserved in massive sulfide ores may be a product of recrystallization of early formed amorphous silica and chalcedony, or late-stage infilling by quartz at higher pH. The existence of a 'quartz solubility window' between ~200 and 350 °C is important for the development of high-grade massive sulfide deposits; otherwise, the base metals, which are deposited in the same temperature range, would be diluted by massive amounts of quartz gangue. In contrast, quartz deposition in the higher temperature stockwork zones of the deposits may occur as a result of rapid depressurization of the fluid as it rises toward the seafloor, or by superheating of the fluid beyond the quartz solubility maximum (**Figure 7**).

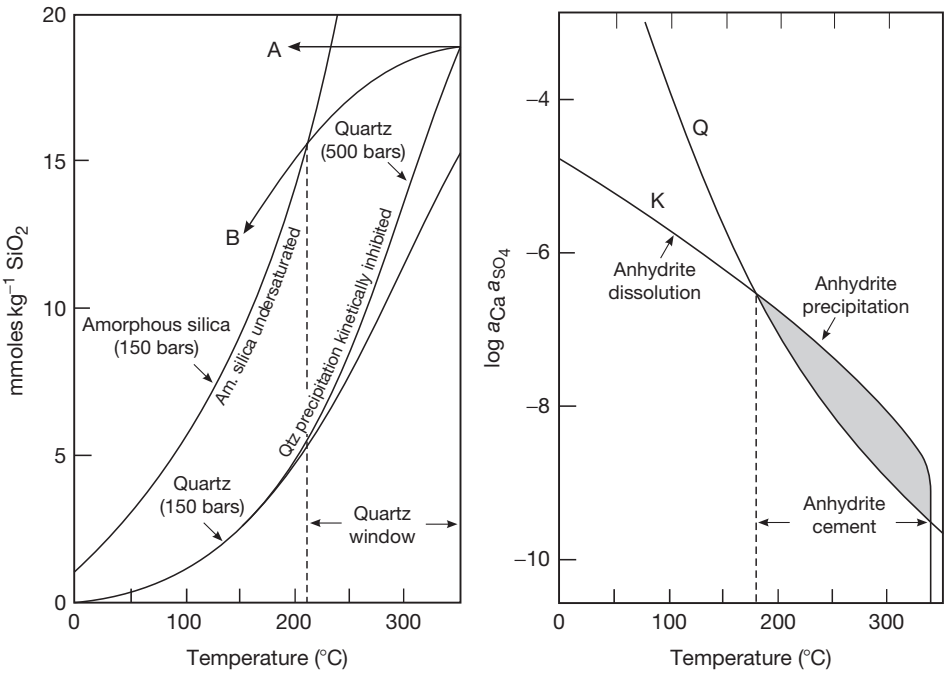

Figure 14 Solubility of amorphous silica and quartz at 500 and 150 bars (left panel). Quartz precipitation is kinetically inhibited at high temperatures, and saturation with amorphous silica occurs only after significant conductive cooling (path A) or a combination of mixing and conductive cooling (path B), creating a 'window' between about 350 and 200 °C during which metals are deposited but not diluted by quartz or amorphous silica. The depicted starting concentration of SiO_2 is the minimum concentration shown in **Figure 7**. Precipitation of anhydrite (right panel) occurs in this same temperature range, cementing the massive sulfides, but it dissolves at lower temperature due to retrograde solubility. Reproduced from Hannington MD, Jonasson I, Herzig P, and Petersen S (1995) Physical and chemical processes of seafloor mineralization at mid-ocean ridges. In: Humphris SE, Zierenberg RA, Mullineaux LS, and Thomson RE (eds.) *Seafloor Hydrothermal Systems: Physical, Chemical, Biological, and Geological Interactions, Geophysical Monograph Series*, vol. 91, pp. 115–157. Washington, DC: American Geophysical Union.

Anhydrite is the principal nonsulfide mineral in black smoker chimneys on the modern seafloor. Although anhydrite ($CaSO_4$) is stable at temperatures above about 150 °C (Figure 14), it is most commonly precipitated with Cu–Fe-sulfides at temperatures close to 350 °C. Because of its retrograde solubility, anhydrite dissolves back into seawater at seafloor pressures when temperatures drop below 150 °C. Hence, it does not dilute the ores and commonly is not preserved in many ancient VMS deposits. In contrast, barite ($BaSO_4$) is highly insoluble in seawater and readily coprecipitates with sulfides in response to mixing between Ba-rich hydrothermal fluids and cold, SO_4-rich seawater. Barite is most abundant in deposits developed above felsic volcanic rocks or sediments that provided an enriched source of Ba. A number of Fe and Mg silicates (notably chlorite) may also precipitate with the sulfides directly from the hydrothermal fluids. Fe-rich chlorite forms at high temperatures (~300–400 °C) under conditions that involve little or no mixing with seawater; Mg-rich chlorite is formed by mixing between the hydrothermal fluids and Mg-rich seawater, generally at lower temperatures and outside the main upflow zone.

Extensive carbonate deposition may result simply from geothermal heating of seawater in shallow-circulating hydrothermal systems (Rimstidt, 1997). However, the abundance of Fe-, Mg-, and Mn-bearing carbonates in many deposits suggests that the ore-forming fluids were also close to CO_2 saturation. At low concentrations of H_2S, siderite may be an important Fe-bearing mineral in the massive sulfide ores, and siderite iron formations are common in the upper parts of many VMS systems. At low aO_2 and low H_2S/CO_2, the stability of siderite is largely independent of pH, forming readily under acidic conditions close to pyrite–pyrrhotite equilibrium. High dissolved CO_2 concentrations may reflect exchange with CO_2-rich source rocks (e.g., remobilization of carbonate from altered ultramafics) or degassing of volatiles from a subvolcanic magma. Boiling also may be a mechanism for the precipitation of carbonate in some VMS deposits (e.g., Rimstidt, 1997).

13.18.8 Alteration Mineralogy and Geochemistry

Most VMS deposits are underlain by extensively altered volcanic rocks in pipe-like or stratabound zones that contain the subseafloor stockwork mineralization. The alteration is produced by reaction of the ore-forming fluids with the host rocks and by entrainment of seawater into the upflow zone. The dominant alteration phases are quartz, muscovite, chlorite, and carbonate (so-called propylitic alteration) typical of the greenschist facies, and less commonly talc, actinolite, biotite, chloritoid, stilpnomelane, and leucoxene. Secondary minerals in the upflow zone are produced mainly by the hydrolysis of feldspar, the loss of sodium and calcium, and by addition of iron, magnesium, and potassium. The formation of chlorite-rich rocks in the pipe-like alteration zones requires substantial removal of silica. In some cases, removal of aluminum can also result in the transformation of chlorite to talc. Where the major cations are completely stripped from the rock, a distinctive aluminous alteration assemblage is produced (e.g., kaolinite–pyrophyllite or muscovite–andalusite in higher grade metamorphic rocks). This aluminous assemblage is particularly evident in deposits that are considered to have been formed from highly acidic fluids with a large magmatic volatile content (Hannington et al., 1999b; Sillitoe et al., 1996).

Alteration pipes beneath Cu–Zn deposits typically have a chloritic core (dominantly Fe-rich chlorite) and sericitic outer zone, whereas alteration beneath Zn–Pb–Cu deposits is commonly dominated by quartz and muscovite. This difference mainly reflects the higher temperatures of the hydrothermal fluids in the upflow zones of Cu–Zn deposits and also the composition and the permeability of the host volcanic rocks. Alteration also causes the rocks surrounding the discharge zone to become insulated, sealing the system against the ingress of seawater and allowing higher temperature fluids to occupy the alteration pipe. This can result in a strong zonation between Fe-rich chlorite in the core of the alteration pipe and Mg-rich chlorite at its margins, caused by the highly restricted flow of high-temperature Fe-rich fluids in the center of the pipe and drawdown of Mg-rich seawater at the cooler, outer margins. Under certain conditions, the Fe content of the chlorite is a useful geothermometer, increasing sharply with temperature (e.g., de Caritat et al., 1993). The mineralogical complexity of the alteration generally decreases with increasing temperature and water/rock ratio (e.g., Figure 15), so that the most intensely altered rocks consist only of quartz and/or chlorite. Where carbonate is abundant, the composition of the carbonate minerals mimics that of chlorite, with Fe-rich carbonate (siderite) occurring in the core of the upflow and in the massive sulfides, and Mg-rich carbonate (ankerite and dolomite) at the margins. The Mn content of carbonate also increases toward the discharge zone.

Three main types of silicification are recognized: silica deposition as a result of conductive cooling of the hydrothermal fluids near the site of discharge (e.g., commonly as vent-proximal chert; Figure 14), silicification caused by breakdown of the primary igneous minerals and release of silica

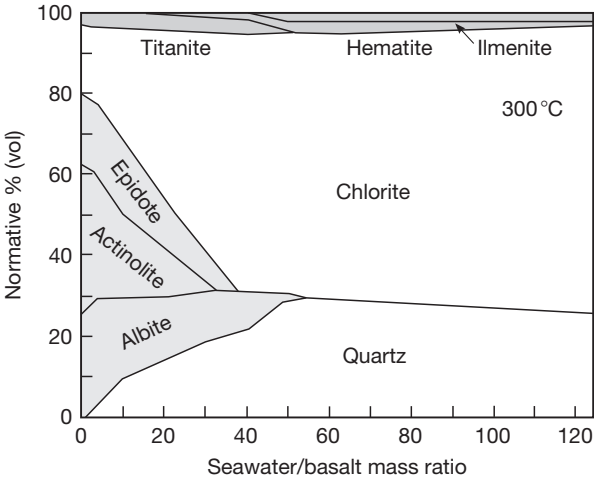

Figure 15 Calculated abundance of alteration minerals formed during seawater–basalt interaction at progressively higher water/rock mass ratios. Alteration mineral assemblages dominated by only quartz and chlorite are indicative of alteration at very high water/rock mass ratios in the upflow zones of the hydrothermal system. Adapted from Mottl MJ (1983) Metabasalts, axial hot springs, and the structure of hydrothermal systems at mid-ocean ridges. *Geological Society of America Bulletin* 94: 161–180.

(e.g., during formation of chlorite), and silica dumping where temperatures exceed the solubility maximum of quartz (Figure 7). A siliceous core zone is common at the top of the alteration pipe, where all three of these processes may contribute to the formation of amorphous silica or quartz.

Chemical changes in the altered rocks are dominated by the Fe enrichment in the core of the upflow zone, K_2O and MgO addition at the margins of the upflow zone, and loss of CaO and Na_2O throughout, corresponding respectively to the formation of Fe- and Mg-chlorite and muscovite and the breakdown of Na- and Ca-bearing plagioclase. A variety of reactions can be written to describe the dominant mass changes in the footwall alteration pipe. All involve hydrolysis or hydration of the rock, major cation exchange (loss of Na and addition of K, Mg, or Fe) and, in the case of chloritization, the loss of Si (e.g., as H_4SiO_4 (aq)):

$$3NaAlSi_3O_8 + K^+ + 2H^+ \rightarrow KAl_3Si_3O_{10}(OH)_2 + 6SiO_2 + 3Na^+$$
$$\text{Albite} \rightarrow \text{Muscovite} + \text{Quartz} \qquad [5]$$

$$2NaAlSi_3O_8 + 3Mg^{2+} + 2Fe^{2+} + 14H_2O \rightarrow Mg_3Fe_2Al_2Si_3O_{10}(OH)_8 + 3H_4SiO_4(aq) + 2Na^+ + 8H^+$$
$$\text{Albite} \rightarrow \text{Chlorite} \qquad [6]$$

This alteration can be mapped using a variety of chemical alteration indices that track the breakdown of plagioclase (e.g., Ishikawa Index $= 100(MgO + K_2O)/(MgO + K_2O + CaO + Na_2O)$; Ishikawa et al., 1976). In the upflow zones, nearly every minor and trace element is leached to some extent, except the least mobile elements such as Ti and Zr. Some easily leachable elements, such as Sr, are quantitatively removed. The concentrations of the immobile elements in the altered rock allow the calculation of net mass gains and losses, for example, using methods such as those of Gresens (1967).

Alteration is not restricted to discordant pipes beneath the deposits but also commonly occurs in stratabound zones, typically confined to permeable fragmental rocks at or near the ore horizon. In contrast to alteration pipes, fluids within these zones diffuse laterally away from the main upflow, mixing with seawater in the permeable strata and forming broad, stratabound, and generally lower temperature alteration assemblages (e.g., Galley, 1993; Large, 1992). Hanging-wall alteration is produced by late-stage hydrothermal fluids that penetrate volcanic rocks or sediment that have buried still-active hydrothermal systems. In some cases, the hanging-wall alteration is related to another younger deposit stratigraphically higher in the volcanic pile (i.e., in a stacked hydrothermal system; Figure 13). In this case, the hanging-wall alteration, which extends above one deposit and terminates at the base of another, is mineralogically and chemically identical to a footwall alteration pipe. In other cases, the hanging-wall alteration is more subtle, caused by spent fluids that leaked into the overlying rocks with relatively little chemical change.

Where the proximal alteration is metamorphosed, it may be quite conspicuous in outcrop, with the dominant muscovite and chlorite assemblages converted to coarse-grained cordierite, biotite, anthophyllite, garnet, andalusite, kyanite, or staurolite (e.g., see Chapter 13.7). Spotted hornfels is also common in the contact aureole of later intrusions that may cut the alteration zones. The metamorphic mineral assemblage is chemically quite similar to the altered volcanic precursor, including trace element enrichments and depletions. For example, mica schists developed from quartz–muscovite alteration zones are commonly fuchsitic, with mineral compositions reflecting the compositions of the altered volcanic rocks (e.g., F, V, or Cr-rich). Garnet-rich zones derived from chloritized mafic or felsic volcanic rocks are commonly manganiferous.

Because of the immense scale of hydrothermal convection systems in large volcanic complexes, the alteration is commonly mappable as regional semiconformable zones (e.g., Brauhart et al., 2001; Skirrow and Franklin, 1994; Figure 16). In mafic volcanic rocks, this regional semiconformable alteration ranges from diagenetic–zeolitic, through carbonate alteration, and spilitization in the upper zones, to silicification and epidote–quartz alteration in the lower zones. Alteration close to the subvolcanic intrusion marks the highest temperature aquifer or reservoir zone for the ore-forming hydrothermal fluids. Here, the major secondary minerals include albite (after calcic plagioclase), actinolite (after pyroxene), and quartz and epidote, commonly in veins and patches that have replaced the whole rock (so-called epidosite; Harper, 1999). Substantial gains of Na and Ca accompany the losses of metals from these rocks. Significant gains in silica (as quartz) occur where the temperatures of the fluids near the top of the reservoir zone exceed the quartz solubility maximum (Figure 7). These zones of silicification can be mapped for many kilometers (e.g., Galley, 1993) and may have acted as an impermeable barrier to high-temperature upflow, causing the ore-forming fluids to become focused into crosscutting structures leading to the seafloor (e.g., synvolcanic fault zones and dike swarms).

13.18.9 Chemical Sediments

A common product of the discharge of hydrothermal fluids at the seafloor is a chemical sediment that flanks or overlies the massive sulfide deposits. The chemical sediments, also referred to as 'exhalites,' are formed from a wide range of hydrothermal products that occur as thin but laterally extensive deposits up to tens of kilometers distant from the vent complex. They include all four common facies of iron formation (sulfide, oxide, carbonate, and silicate), pyritic chert, manganiferous shales, and altered tuffaceous sediment. Commonly, the sediments have a clastic (e.g., tuffaceous) component in addition to the chemically precipitated hydrothermal minerals. Franklin et al. (2005) cautioned that the association of iron formation with VMS deposits is not ubiquitous and may be incidental in some cases. Bedded barite is also common in some Zn–Pb–Cu deposits.

Three dominant mechanisms of formation of chemical sediments associated with VMS deposits have been proposed: direct chemical precipitation from hydrothermal fluids that are vented into a stratified water column or brine pool, fallout of particulate material (especially Fe sulfides, Fe oxides, and Mn oxides) from a buoyant hydrothermal plume, and low-temperature diffuse flow of hydrothermal fluids through fine-grained volcaniclastic rocks or other sediments at or near the seafloor. Deposition of chemical sediments can precede, be synchronous with, or postdate the formation of the massive sulfide deposits.

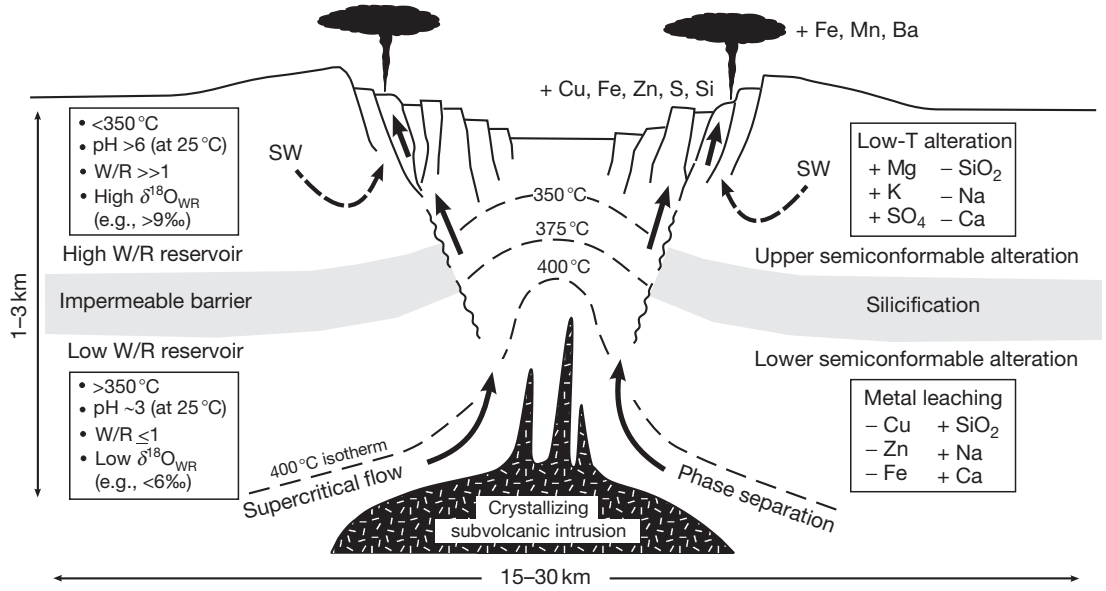

Figure 16 Summary of the main features of convective hydrothermal systems responsible for forming VMS deposits, including compositions of hydrothermal fluids in the recharge zone and high-temperature reaction zone, major mass gains and losses of elements in different parts of the hydrothermal alteration system, and the distribution of large-scale semiconformable alteration zones. Reproduced from Galley AG (1993) Semi-conformable alteration zones in volcanogenic massive sulfide districts. *Journal of Geochemical Exploration* 48: 175–200; Franklin JM, Gibson HL, Jonasson IR, and Galley AG (2005) Volcanogenic massive sulfide deposits. In: Hedenquist JW, Thompson JFH, Goldfarb RJ, and Richards JP (eds.) *100th Anniversary Volume of Economic Geology*, pp. 523–560. Littleton, CO: Society of Economic Geologists.

Because the fluids are warm and enriched in reduced iron and sulfur, they may have contributed to bacterial growth, which is reflected in ancient chemical sediments by a large carbonaceous component. Filamentous bacteria are also recognized as an important substrate for the deposition of amorphous silica in associated chert beds. Distal oxide-facies (hematite and magnetite) iron formation is most commonly associated with VMS deposits hosted by mixed volcanic and sedimentary sequences, such as in the Bathurst mining camp of New Brunswick. Chlorite or siderite may also be important hydrothermal constituents of these chemical sediments. Cherty hematite (jasper) and sulfide-rich iron formation, such as that associated with the Kuroko deposits of Japan (i.e., tetsusekiei), commonly occur close to the deposits. Albite, apatite, tourmaline, and other Fe silicate minerals (e.g., stilpnomelane) are also common constituents of exhalites associated with different VMS deposits.

The chemical composition of the sediments can be a useful indicator of proximity to hydrothermal upflow zones (e.g., enrichments in Fe, Mn, Pb, and Zn and, in particular, ratios of these elements to clastic components in the sediment indicated by Al and Ti; Peter and Goodfellow, 2000; Spry et al., 2000). The compositions of the sediments are also sensitive indicators of deepwater conditions, including ambient temperature, aO_2, H_2S content, and silica content (Grenne and Slack, 2003, 2005; Slack et al., 2007). The rare earth element (REE) geochemistry, in particular, may be an indicator of redox and proximity to high-temperature hydrothermal upflow. Because Eu can exist in the 2+ valence state it is effectively transported in reduced hydrothermal fluids, especially at elevated temperatures (Bau, 1991), and thus can be enriched in ore-forming solutions. Chemical sediments formed from these solutions commonly have REE profiles with positive Eu anomalies, reflecting the enrichment in Eu^{2+} relative to the other lanthanides.

13.18.10 Sulfur Isotopes

The isotopic composition of sulfur in VMS deposits reflects the different sources of reduced and oxidized sulfur and the variability in the sulfur isotopic composition of seawater through time since the Precambrian (e.g., **Figure 17**). The $\delta^{34}S$ values of sulfides in Precambrian VMS deposits are typically close to 0‰, with a much smaller range than in Phanerozoic deposits. The latter closely parallel the isotopic composition of contemporaneous seawater sulfate, with the sulfide minerals being 17.5 ± 2.5‰ lighter than coeval seawater (e.g., Huston, 1999; Sangster, 1968). This difference is close to the isotopic fractionation between aqueous sulfur and sulfide at temperatures between 250 and 400 °C (25–19‰; Ohmoto and Goldhaber, 1997). However, in most cases aqueous sulfide and sulfate did not equilibrate chemically (or isotopically) during formation of the deposits. Thus, the isotopic differences between sulfide and sulfate minerals mainly reflect the different sources (i.e., leached igneous sulfide and seawater sulfate). Within some deposits there is a progressive shift in the isotopic composition of sulfur with ore type or stratigraphic position, which may reflect either contributions from the different sources of sulfur or changing physical and chemical conditions during mineralization (e.g., temperature, pH, aO_2; Ohmoto and Goldhaber, 1997).

Analyses of modern vents indicate that $\delta^{34}S$ values of hydrogen sulfide, from 1‰ to 7‰, represent mainly leached sulfur from the basaltic substrate, with <10% contribution

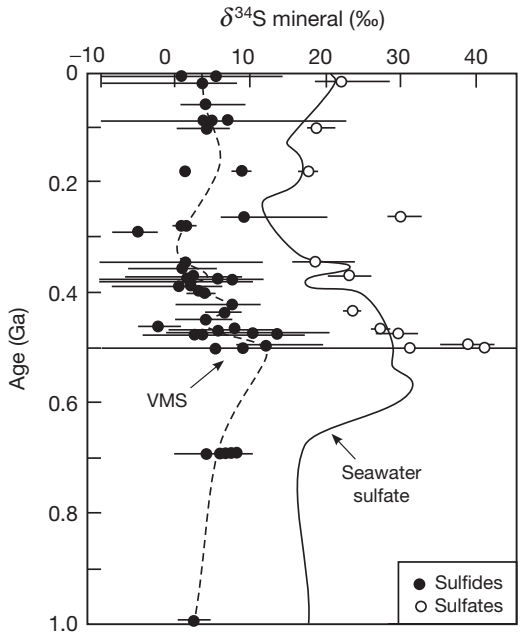

Figure 17 Sulfur isotope composition of sulfide and sulfate minerals in VMS deposits. The data include the mean $\delta^{34}S$ value for different VMS districts (symbol) and the range (horizontal lines). A dashed line fitted through the district mean values generally matches the pattern of the seawater evolution curve ($\delta^{34}S$ of sulfate) over the last 1.0 Ga. Redrawn from Huston DL (1999) Stable isotopes and their significance for understanding the genesis of volcanic-hosted massive sulfide deposit: A review. *Reviews in Economic Geology* 8: 157–179.

from inorganically reduced seawater sulfate (Shanks, 2001). Although the bulk of the ore fluid is hydrothermally modified seawater, most of the seawater sulfur is exchanged for igneous sulfur from the crust. This has been uniquely confirmed by analyses of multiple sulfur isotopes (e.g., ΔS^{33}; Ono et al., 2007). Deposits that occur in mafic-dominated settings typically have $\delta^{34}S$ values slightly higher (i.e., 0–2‰) than that of mantle sulfur. Deposits hosted by felsic or sedimentary rocks, or where basement rocks may include older crust, commonly have $\delta^{34}S$ values that are more variable. Somewhat higher $\delta^{34}S$ values for arc lavas (4–10‰), compared to mid-ocean ridge basalt (0.1 ± 0.5‰), are interpreted to be mainly due to subducted seawater sulfate that was recycled by arc magmatism (e.g., Alt et al., 1993). This process may account for the previously recognized difference in the sulfur isotopic compositions of mafic-dominated Cu–Zn and felsic-dominated Zn–Pb–Cu deposits (Lydon, 1984). High $\delta^{34}S$ values in a number of sediment-hosted deposits likely reflect seawater sulfate reduction by reaction with sedimentary organic matter. However, a wide range of sulfur isotope values is recorded, including both heavy sulfur and very light sulfur indicative of bacterial sulfate reduction (Böhlke and Shanks, 1994; Zierenberg, 1994). Anomalously low $\delta^{34}S$ values also have been found in VMS deposits with abundant high-sulfidation sulfide mineral assemblages and aluminous alteration discussed above. These values have been interpreted to indicate the direct input of volcanic SO_2 in the hydrothermal fluids (e.g., Hannington et al., 1999b). Volcanic SO_2 is the predominant sulfur gas at magmatic temperatures, but at temperatures below 300 °C, the SO_2 disproportionates rapidly to form mainly H_2S and H_2SO_4, accompanied by a large equilibrium isotopic fractionation that produces the low $\delta^{34}S$ values of H_2S (Rye, 1993).

13.18.11 Oxygen, Hydrogen, and Carbon Isotopes

Oxygen and hydrogen isotope ratios of fluid inclusions in ore minerals from numerous Phanerozoic VMS deposits are consistent with the interpretation that the ore solutions were modified seawater. The data from ancient deposits also suggest that the isotopic composition of seawater has been relatively constant over time, with $\delta^{18}O$ and δD values both close to 0‰. δD and $\delta^{18}O$ values of H_2O in modern vent fluids are within a few per mil of seawater values, with small deviations resulting from water–rock interaction at variable temperatures or small contributions of magmatic water (Shanks, 2001). A somewhat larger range of isotopic compositions for ore-forming fluids has been calculated from the isotopic compositions of hydrothermal minerals (especially quartz), including $\delta^{18}O$ values of H_2O ranging from -2 to $+4$‰ and δD values from -30 to $+10$‰ (Huston, 1999). These values imply significant isotopic exchange with altered rock, but may also reflect mixing of fluids of different origin or boiling (e.g., **Figure 18**). $\delta^{18}O$ and δD values of plausible magmatic fluids in VMS environments range from 6 to 10‰ and -35 to -50‰, respectively, which would shift the isotopic compositions of the ore-forming fluids to higher $\delta^{18}O$ and lower δD values. Boiling also can shift the isotopic compositions of the fluids to higher $\delta^{18}O$ and lower δD values, but the lowest δD values are commonly interpreted to record contributions of magmatic water.

As hydrothermal fluids react with volcanic rocks, the isotopic composition of the whole rock also shifts. Volcanic rocks have higher $\delta^{18}O$ values (typically in the range of 6–10‰) than the ore-forming fluids. Therefore, whole-rock oxygen isotope values that are notably lower than those of unaltered rocks indicate where reactions took place at high temperatures and low water/rock ratios (**Figure 18**). The alteration zones are typically characterized by a core zone of low $\delta^{18}O$ values, reflecting a high-temperature reaction with the ore-forming fluids, with significantly higher $\delta^{18}O$ values in the surrounding rocks recording low temperatures distal to the ore. Regionally, the lowest $\delta^{18}O$ values are found closest to the contact with the ore-related subvolcanic intrusions (e.g., Cathles, 1993) and reflect the conditions that would have been most suitable for metal leaching (i.e., very low water/rock ratios of 1–10 and high temperatures). Higher $\delta^{18}O$ values in rocks above this zone indicate exchange at high water/rock ratios and relatively lower temperatures (**Figure 16**). As a result, whole-rock oxygen isotope data are useful for mapping the paleogeothermal gradients in the large-scale alteration zones.

$\delta^{13}C$ values of carbonate minerals in VMS deposits have a relatively restricted range from -7 to 0‰ (Huston, 1999). These values have been attributed to derivation from seawater bicarbonate, which has a $\delta^{13}C$ value close to 0‰, regardless of age (Ohmoto and Goldhaber, 1997). Carbon dioxide $\delta^{13}C$ values in the majority of modern seafloor vents are between -4 and -9‰ and are interpreted to reflect mainly volcanic or 'mantle' sources (e.g., Von Damm, 1990). Thus, carbonate $\delta^{13}C$ values in most VMS deposits are consistent with either a

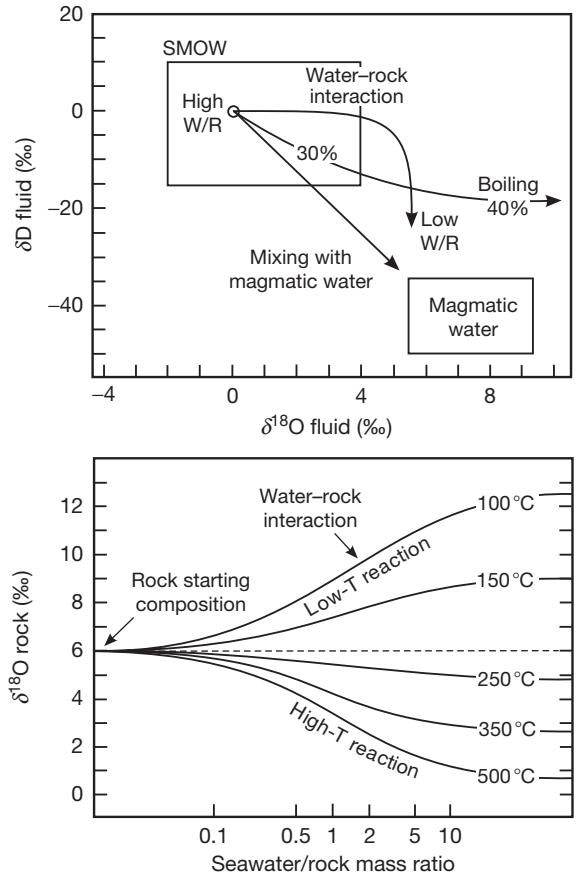

Figure 18 Schematic illustration of the isotopic composition of evolved hydrothermal fluids (upper panel), showing a number of possible pathways for increasing $\delta^{18}O$ and decreasing δD values relative to standard mean ocean water (SMOW). Adapted from Huston DL (1999) Stable isotopes and their significance for understanding the genesis of volcanic-hosted massive sulfide deposit: A review. *Reviews in Economic Geology* 8: 157–179. The lower panel shows modeled whole-rock $\delta^{18}O$ values for volcanic rocks with a starting composition of 6‰ following alteration at high and low temperatures by hydrothermal seawater. Adapted from Paradis S, Taylor BE, Watkinson DI, and Jonasson IR (1993) Oxygen isotope zonation and alteration in the northern Noranda district, Quebec: Evidence for hydrothermal fluid flow. *Economic Geology* 88: 1512–1525, using data from O'Neil and Taylor, 1967.

seawater or volcanic source for the carbon. $\delta^{18}O$ values of carbonate have a much larger range that does not correlate with $\delta^{13}C$ and most likely indicates variable temperatures of carbonate deposition, in the range of 100–300 °C. Graphitic carbon, which is a common component of ore-related sedimentary rocks, typically has $\delta^{13}C$ values in the range of -35 to -20‰ that are attributed to the role of thermophilic bacteria in the generation of precursor methane with very low $\delta^{13}C$ values (e.g., Shanks, 2001). However, $\delta^{13}C$ values in the range of -9 to -26‰ in some modern seafloor vents also have been interpreted to reflect abiogenic CH_4 production at high temperatures. Very low $\delta^{13}C$ values are also common in carbonates from sediment-hosted massive sulfide deposits, resulting from the oxidation of reduced organic carbon in the sediments (e.g., Goodfellow and Zierenberg, 1999).

13.18.12 Strontium and Lead Isotopes

Strontium isotopes of sulfate minerals in VMS deposits (e.g., barite, carbonate, gypsum, and anhydrite) and in altered whole rocks invariably record a mixture of Sr derived from seawater and Sr leached from the underlying volcanic rocks, as well as variation in the isotopic composition of seawater Sr over time. Minerals precipitated directly from seawater have $^{87}Sr/^{86}Sr$ values that are somewhat lower than coeval seawater, indicating a small contribution of Sr leached from volcanic rocks. Strontium isotope data for modern vent fluids (Von Damm, 1990) indicate a predominantly basaltic source for Sr, with small contributions from seawater. Spooner et al. (1977) first noted that the altered rocks of the Troodos ophiolite of Cyprus were enriched in ^{87}Sr and concluded that hydrothermal seawater was the altering fluid because it was the only available reservoir with a high enough $^{87}Sr/^{86}Sr$ ratio. The strontium isotope ratios of basalts that have equilibrated with seawater at high temperatures also provide an indication of the bulk water/rock ratio.

Lead isotope data for sulfides indicate a predominantly volcanic source for the Pb in VMS deposits. As a rule, the narrow range of Pb isotope values for a VMS district suggests that metal-rich fluids formed from the leaching of a homogeneous basement source. Differences between districts and between deposits of different ages are related to compositional variations in the basement and evolution of the mantle source for the host volcanic rocks in each district. The Pb isotope signatures of galena in Precambrian Cu–Zn deposits are typically quite primitive, whereas radiogenic Pb is more abundant in younger deposits and especially in deposits with U- and Th-enriched source rocks such as continental crust or sedimentary rocks. As a result, Pb isotope data for most Archean Cu–Zn deposits plot close to the mantle evolution line, whereas Phanerozoic Zn–Pb–Cu deposits are closer to or above the orogene curve (Franklin et al., 1981). Although most Archean and Early Proterozoic deposits have Pb isotope signatures that are similar to MORB-like mantle sources, a few of the oldest known deposits, for example in the Pilbara and Slave provinces, have somewhat more radiogenic Pb indicating a source that had a longer upper crustal history (Thorpe, 1999). This is also reflected in the bulk compositions of the deposits, which are unusually Pb- and Ag-rich compared to other Archean VMS.

13.18.13 Conclusions

A number of aspects of VMS deposits, including their mineralogy, compositions of the underlying rocks, and stable and radiogenic isotope tracers, are consistent with metals and sulfur being derived mainly by leaching of volcanic rocks stratigraphically below the deposits. Cu–Zn deposits occur above rock successions composed predominantly of mafic volcanic rocks or their derivatives, whereas Zn–Pb–Cu deposits occur above felsic volcanic and/or sedimentary rock successions. The common spatial and temporal association of VMS deposits with felsic volcanism mainly reflects the high heat flow and partial melting of the crust during rifting, but also can be interpreted in terms of direct magmatic contributions to the hydrothermal fluids from the felsic magmas. While the nature

of the source rocks and their parent magmas is an important determinant of the bulk compositions of the deposits, the proportions of metals and metal zoning are also a result of temperature-dependent solubilities of the ore metals in the hydrothermal solutions. Although the bulk of the sulfur, like the metals, was derived by subseafloor leaching, a portion of the reduced sulfur may include a component of seawater sulfate that was reduced to sulfide during interaction with ferrous iron components in the volcanic rocks or by biogenic reduction at the site of deposition of the metals.

The average VMS deposit contains at least 4×10^7 kg of Cu and 8×10^7 kg of Zn (e.g., geometric mean size and grades of bimodal mafic deposits; **Table 1**). In a leaching model, this requires a source region of only $\sim$1 km^3, if the rocks contain 100 ppm combined Cu and Zn (e.g., basaltic basement) and 100% of the metal is extracted and deposited in the massive sulfides. However, the extent of leaching, and especially the efficiency of deposition, is generally far smaller. A more reasonable estimate would involve a source capable of contributing as much as $10\times$ this amount of metal. Large zones of semiconformable alteration, which may be of the order of 100 km^3, are the most likely source for these metals, and the amount of metal leached from these rocks more than accounts for the metal contained in the associated deposits (Brauhart et al., 2001; Richardson et al., 1987; Skirrow and Franklin, 1994). However, for large or high-grade deposits, the quantity of metal involved may require unrealistically large volumes of rock as the source (e.g., Yang and Scott, 2006). The total metal endowment and notable enrichments of certain trace elements (e.g., Bi, Se, In, and Sn) also argue strongly for a magmatic contribution to these deposits.

Another important constraint is the size of the subvolcanic heat source, which must have been large enough to circulate the volume of hydrothermal fluid needed to form the deposits. Assuming a concentration of only 1–5 ppm Cu and 5–10 ppm Zn in the fluid, the average deposit would require a total flux of high-temperature fluid of more than 1×10^{14} kg to account for the contained metal. The heat required to raise the temperature of 1 kg of seawater to 350 °C requires a magmatic intrusion of approximately the same mass (Cathles et al., 1983); therefore, a subvolcanic heat source of at least 100 km^3 would be needed. A much larger heat source is needed in most cases because only a small fraction of the seawater heated to 350 °C actually arrives at the seafloor at this temperature (e.g., Elderfield and Shultz, 1996). While this magma is not necessarily emplaced all at one time, these observations cast some doubt on the ability of a convective hydrothermal system to provide all of the metals, especially for the largest and richest deposits. As a result, many researchers have concluded that other sources of metals must be involved (e.g., Large et al., 1996; Scott, 1997; Stanton, 1990, 1994; Urabe, 1987; Yang and Scott, 2006).

Limited oxygen and hydrogen isotope data confirm that direct contributions of magmatic water have occurred in some arc and back-arc hydrothermal systems (Gamo et al., 1997; Marumo and Hattori, 1999). However, we are only just beginning to understand the processes involved in transferring metal-rich brines from the magmas to the hydrothermal fluids. Brine inclusions of probable magmatic derivation in subseafloor plutonic rocks contain daughter minerals of pyrite and chalcopyrite that indicate metal concentrations of up to 1000s of ppm Fe and Cu in the trapped fluids (de Ronde, 1995; Kelley and Delaney, 1987). Only a small contribution from such brines, mixed with modified seawater, can account for major metal concentrations in the vent fluids. In some arc lavas, CO_2-rich inclusions containing high concentrations of Cu-, Fe-, and Zn-chlorides also have been found (Kamenetsky et al., 2001; Yang and Scott, 1996, 2002).

The processes responsible for the formation of VMS deposits have been much the same since the Precambrian, but certain time periods in the geologic past were particularly favorable for their formation and preservation. Major peaks in deposit formation correlate with episodes of crustal growth and assembly of the continental landmasses, as well as with episodes of global ocean anoxia (Groves and Barley, 1994; Holland, 2004, 2005). Some of the genetic models proposed for deposits that formed during these episodes do not apply to younger VMS deposits or to conditions on the seafloor today. For example, some large VMS deposits are believed to have formed by the accumulation of metals in stagnant, anoxic basins from the fallout of particulates in buoyant hydrothermal plumes. This style of mineralization does not occur in the modern oceans because of the rapid dispersal and oxidation of plume particles. Although textures reminiscent of black smokers have been recognized in deposits as old as 3.2 Ga (Vearncombe et al., 1995), chimney structures typical of modern VMS deposits are not preserved in these. In the early Precambrian, anhydrite was virtually absent in massive sulfide deposits because of the generally reduced nature of the Precambrian oceans and the absence of SO_4 in deep seawater. This, together with metamorphism, may explain why most Precambrian VMS deposits lack evidence of large fossil chimney structures like those at modern seafloor vents that owe their stability to anhydrite cement.

An important feature of modern seafloor hydrothermal systems that is slowly being revealed in ancient deposits is evidence of a diverse fossil vent fauna. Fossilized remnants of vent organisms such as vestimentiferan tubeworms have been documented in deposits as old as the early Paleozoic (e.g., Little et al., 1998). Evidence of fossil life in still older VMS deposits is less compelling but still found. The widespread occurrence of carbonaceous or graphitic sedimentary rocks associated with massive sulfide deposits of much earlier times, including in the Early Archean, raises the possibility that chemoautotrophic bacteria were abundant at Archean seafloor hydrothermal vents. Studies of possible fossil bacteria in Archean iron formations, in particular, have highlighted the importance of seafloor hydrothermal activity in the evolution of early life (Rasmussen, 2000; Russell et al., 2005; Schopf, 1993). Thus, research on ancient VMS deposits is likely to figure prominently in our future understanding of the origins of life on Earth and even the possibility of life on other planets (e.g., Nisbet and Sleep, 2001; Shock and Schulte, 1998; Schulte et al., 2006).

Acknowledgments

This article draws on two landmark publications on the geology of VMS deposits that are contained in the 75th (1981) and 100th (2005) Anniversary Volumes of *Economic Geology*,

coauthored by Jim Franklin, Don Sangster, John Lydon, Harold Gibson, Alan Galley, and Ian Jonasson; and on the work of Ross Large and David Huston. John Slack and David Huston provided very helpful reviews of an early version of this manuscript that greatly improved this contribution.

References

Alt JC (1995) Subseafloor processes in mid-ocean ridge hydrothermal systems. In: Humphris SE, Zierenberg RA, Mullineaux LS, and Thomson RE (eds.) *Seafloor Hydrothermal Systems: Physical, Chemical, Biological, and Geological Interactions, Geophysical Monograph Series*, vol. 91, pp. 85–114. Washington, DC: American Geophysical Union.

Alt JC, Laverne C, Vanko DA, et al. (1996) Hydrothermal alteration of a section of upper oceanic crust in the eastern Equatorial Pacific; synthesis of results from Site 504, DSDP legs 69-70, and 83, and ODP legs 111, 137, 140, and 148. In: Alt JC, Kinoshita H, Stokking LB, and Michael PJ (eds.) *Proceedings of the Ocean Drilling Program. Scientific Results*, vol. 148, pp. 417–434. College Station, TX: Ocean Drilling Program.

Alt JC and Shanks WC III (2003) Serpentinization of abyssal peridotites from the MARK area, Mid-Atlantic ridge: Sulfur geochemistry and reaction modeling. *Geochimica et Cosmochimica Acta* 67: 641–653.

Alt JC, Shanks WC III, and Jackson MC (1993) Cycling of sulfur in subduction zones: The geochemistry of sulfur in the Mariana island arc and back-arc trough. *Earth and Planetary Science Letters* 119: 477–494.

Auclair G, Fouquet Y, and Bohn M (1987) Distribution of selenium in high-temperature hydrothermal sulfide deposits at 13°N, East Pacific Rise. *The Canadian Mineralogist* 25: 577–588.

Barnes HL and Seward TM (1997) Geothermal systems and mercury deposits. In: Barnes HL (ed.) *Geochemistry of Hydrothermal Ore Deposits*, 3rd edn., pp. 699–736. New York: Wiley.

Barrie CT and Hannington MD (1999) Classification of volcanic-associated massive sulfide deposits based on host-rock composition. *Reviews in Economic Geology* 8: 1–11.

Barton PB Jr (1978) Some ore textures involving sphalerite from the Furutobe mine, Akita Prefecture, Japan. *Mining Geology* 28: 293–300.

Barton PB Jr. and Bethke PM (1987) Chalcopyrite disease in sphalerite: Pathology and epidemiology. *American Mineralogist* 72: 451–467.

Barton PB Jr. and Skinner BJ (1979) Sulfide mineral stabilities. In: Barnes HL (ed.) *Geochemistry of Hydrothermal Ore Deposits*, 2nd edn., pp. 278–403. New York: Wiley.

Bau M (1991) Rare-earth element mobility during hydrothermal and metamorphic fluid–rock interaction and the significance of the oxidation state of europium. *Chemical Geology* 93: 219–230.

Bischoff JL and Pitzer KS (1985) Phase relations and adiabats in boiling seafloor geothermal systems. *Earth and Planetary Science Letters* 75: 327–338.

Bischoff JL and Pitzer KS (1989) Liquid-vapor relations for the system NaCl–H_2O: Summary of the P-T-x surface from 300° to 500°C. *American Journal of Science* 289: 217–248.

Bischoff JL and Rosenbauer RJ (1983) A note on the chemistry of seawater in the range 350–500°C. *Geochimica et Cosmochimica Acta* 47: 139–144.

Bischoff JL and Rosenbauer RJ (1984) The critical point and two-phase boundary of seawater, 200–500°C. *Earth and Planetary Science Letters* 68: 172–180.

Bischoff JL and Rosenbauer RJ (1987) Phase separation in seafloor geothermal systems: An experimental study on the effects of metal transport. *American Journal of Science* 287: 953–978.

Bischoff JL and Rosenbauer RJ (1988) Liquid-vapor relations in the critical region of the system NaCl–H_2O from 380 to 415°C: A refined determination of the critical point and two-phase boundary of seawater. *Geochimica et Cosmochimica Acta* 52: 2121–2126.

Bischoff JL and Rosenbauer RJ (1989) Salinity variations in submarine hydrothermal systems by layered double-diffusive convection. *Journal of Geology* 97: 613–623.

Bischoff JL and Seyfried WE Jr. (1978) Hydrothermal chemistry of seawater from 25°C to 350°C. *American Journal of Science* 278: 838–860.

Böhlke JK and Shanks WC III (1994) Stable isotope study of hydrothermal vents at Escanaba trough: Observed and calculated effects of sediment-seawater interaction. In: Morton JL, Zierenberg RA, and Reiss CA (eds.) *Geologic, Hydrothermal, and Biologic Studies at Escanaba Trough, Gorda Ridge, Offshore Northern California. US Geological Survey Bulletin*2022, pp. 223–239. Reston VA: US Geological Survey.

Bourcier WL and Barnes HL (1987) Ore solution chemistry: VII. Stabilities of chloride and bisulfide complexes of zinc to 350°C. *Economic Geology* 82: 1839–1863.

Bowers TS, Campbell AC, Measures CI, Spivack AJ, Khadem M, and Edmond JM (1988) Chemical controls on the composition of vent fluids at 13–11°N and 21°N, East Pacific Rise. *Journal of Geophysical Research* 93: 4522–4536.

Bowers TS, Von Damm KL, and Edmond JM (1985) Chemical evolution of mid-ocean ridge hot springs. *Geochimica et Cosmochimica Acta* 49: 2239–2252.

Brauhart CW, Huston DL, Groves DI, Mikucki EJ, and Gardoll SJ (2001) Geochemical mass-transfer patterns as indicators of the architecture of a complete volcanic-hosted massive sulfide hydrothermal alteration system, Panorama district, Pilbara, Western Australia. *Economic Geology* 96: 1263–1278.

Butterfield DA and Massoth GJ (1994) Geochemistry of north Cleft segment vent fluids: Temporal changes in chlorinity and their possible relation to recent volcanism. *Journal of Geophysical Research* 99: 4951–4968.

Butterfield DA, McDuff RE, Mottl MJ, Lilley MD, Lupton JE, and Massoth GJ (1994) Gradients in the composition of hydrothermal fluids from the Endeavour segment vent field: Phase separation and brine loss. *Journal of Geophysical Research* 99: 9561–9583.

Butterfield DA, Seyfried WE Jr., and Lilley MD (2003) Composition and evolution of hydrothermal fluids. In: Halbach PE, Tunnicliffe V, and Hein JR (eds.) *Energy and Mass Transfer in Marine Hydrothermal Systems*, pp. 123–161. Berlin: Dahlem University Press.

Candela PA and Piccoli PM (2005) Magmatic processes in the development of porphyry-type systems. In: Hedenquist JW, Thompson JFH, Goldfarb RJ, and Richards JP (eds.) *100th Anniversary Volume of Economic Geology*, pp. 25–38. Littleton, CO: Society of Economic Geologists.

Cathles LM (1993) Oxygen isotope alteration in the Noranda mining district, Abitibi greenstone belt, Quebec. *Economic Geology* 88: 1483–1511.

Cathles LM (1997) Thermal aspects of ore formation. In: Barnes HL (ed.) *Geochemistry of Hydrothermal Ore Deposits*, 3rd edn., 191–227. New York: Wiley.

Cathles LM, Erendi AHJ, and Barrie CT (1997) How long can a hydrothermal system be sustained by a single intrusive event? *Economic Geology* 92: 766–771.

Cathles LM, Guber AL, Lenagh TC, and Dudas FO (1983) Kuroko-type massive sulfide deposits of Japan: Products of an aborted island-arc rift. *Economic Geology Monograph* 5: 96–114.

Coumou D, Driesner T, Weis P, and Heinrich CA (2009) Phase separation, brine formation, and salinity variation at black smoker hydrothermal systems. *Journal of Geophysical Research* 114: B03212.

de Caritat P, Hutcheon I, and Walshe JL (1993) Chlorite geothermometry – A review. *Clays and Clay Minerals* 41: 219–239.

de Ronde CEJ (1995) Fluid chemistry and isotopic characteristics of seafloor hydrothermal systems and associated VMS deposits: Potential for magmatic contributions. In: Thompson JFH (ed.) *Magmas, Fluids, and Ore Deposits*. *Mineralogical Association of Canada Short Course Series*, vol. 23, pp. 479–510. Ottawa: Mineralogical Association of Canada.

de Ronde CEJ, Hannington MD, Stoffers P, et al. (2005) Evolution of a submarine magmatic-hydrothermal system: Brothers volcano, southern Kermadec arc, New Zealand. *Economic Geology* 100: 1097–1133.

Ding K and Seyfried WE Jr. (1992) Determination of Fe–Cl complexing in the low pressure supercritical region (NaCl fluid): Iron solubility constraints on pH of subseafloor hydrothermal fluids. *Geochimica et Cosmochimica Acta* 56: 3681–3692.

Doe BR (1994) Zinc, copper, and lead in mid-ocean ridge basalts and the source rock control on Zn/Pb in ocean-ridge hydrothermal deposits. *Geochimica et Cosmochimica Acta* 58: 2215–2223.

Doyle MG and Allen RL (2003) Subsea-floor replacement in volcanic-hosted massive sulfide deposits. *Ore Geology Reviews* 23: 183–222.

Elderfield H and Shultz A (1996) Mid-ocean ridge hydrothermal fluxes and the chemical composition of the ocean. *Annual Review of Earth and Planetary Sciences* 24: 191–224.

Eldridge CS, Barton PB Jr., and Ohmoto H (1983) Mineral textures and their bearing on formation of the Kuroko orebodies. *Economic Geology Monograph* 5: 241–281.

Fontaine FJ and Wilcock WSD (2006) Dynamics and storage of brine in mid-ocean ridge hydrothermal systems. *Journal of Geophysical Research* 111: B06102.

Fouquet Y, von Stackelberg U, Charlou J-L, et al. (1993) Metallogenesis in back-arc environments: The Lau Basin example. *Economic Geology* 88: 2154–2181.

Fournier RO (1985) The behavior of silica in hydrothermal solution. *Reviews in Economic Geology* 2: 45–62.

Foustoukos DI and Seyfried WE Jr. (2007) Fluid phase separation processes in submarine hydrothermal systems. *Reviews in Mineralogy and Geochemistry* 65: 213–239.

Francheteau J, Needham HD, Choukroune P, et al. (1979) Massive deep sea sulphide ore deposit discovered on the East Pacific Rise. *Nature* 277: 523–528.

Franklin JM, Gibson HL, Jonasson IR, and Galley AG (2005) Volcanogenic massive sulfide deposits. In: Hedenquist JW, Thompson JFH, Goldfarb RJ, and Richards JP (eds.) *100th Anniversary Volume of Economic Geology*, pp. 523–560. Littleton, CO: Society of Economic Geologists.

Franklin JM, Lydon JW, and Sangster DF (1981) Volcanic-associated massive sulfide deposits. In: Skinner BJ (ed.) *75th Anniversary Volume of Economic Geology*, pp. 485–627. Lancaster, PA: The Economic Geology Publishing Company.

Galley AG (1993) Semi-conformable alteration zones in volcanogenic massive sulfide districts. *Journal of Geochemical Exploration* 48: 175–200.

Galley AG (2003) Composite synvolcanic intrusions associated with Precambrian VMS-related hydrothermal systems. *Mineralium Deposita* 38: 443–473.

Gamo T, Okamura K, Charlou J-L, et al. (1997) Acidic and sulfate-rich hydrothermal fluids from the Manus back-arc basin, Papua New Guinea. *Geology* 25: 139–142.

Gibson HL (2005) Volcanic-hosted ore deposits. In: Marti J and Ernst GJ (eds.) *Volcanoes and the Environment*, pp. 333–386. Cambridge: Cambridge University Press.

Gillis KM and Banerjee NR (2000) Hydrothermal alteration patterns in supra-subduction zone ophiolites. In: Dilek Y, Moores E, Elthon D, and Nicolas A (eds.) *Ophiolites and Oceanic Crust: New Insights from Field Studies and the Ocean Drilling Program, GSA Special Papers 349*, pp. 283–297. Boulder, CO: Geological Society of America.

Gillis KM, Muehlenbachs K, Stewart M, Gleeson T, and Karson J (2001) Fluid flow patterns in fast spreading East Pacific Rise crust exposed at Hess Deep. *Journal of Geophysical Research* 106: 26311–26329.

Gillis KM, Thompson G, and Kelley DS (1993) A view of the lower crustal component of hydrothermal systems at the Mid-Atlantic Ridge. *Journal of Geophysical Research* 98: 19597–19619.

Gilmour P (1965) The origin of the massive sulfide mineralization in the Noranda district, Northwestern Quebec. *Geological Association of Canada Proceedings* 16: 63–81.

Goodfellow WD and Zierenberg RA (1999) Genesis of massive sulfide deposits at sediment-covered spreading centers. *Reviews in Economic Geology* 8: 297–324.

Grenne T and Slack JF (2003) Paleozoic and Mesozoic silica-rich seawater: Evidence from hematitic chert (jasper) deposits. *Geology* 31: 319–322.

Grenne T and Slack JF (2005) Geochemistry of jasper beds from the Ordovician Løkken ophiolite, Norway: Origin of proximal and distal siliceous exhalites. *Economic Geology* 100: 1511–1527.

Gresens RL (1967) Composition–volume relationships of metasomatism. *Chemical Geology* 2: 47–55.

Groves DI and Barley ME (1994) Archean mineralization. In: Condie KC (ed.) *Archean Crustal Evolution*, *Developments in Precambrian Geology*, vol. 11, pp. 461–503.

Hajash A and Chandler GW (1981) An experimental investigation of high-temperature interactions between seawater and rhyolite, andesite, basalt, and peridotite. *Contributions to Mineralogy and Petrology* 78: 240–254.

Hannington MD, de Ronde CEJ, and Petersen S (2005) Sea-floor tectonics and submarine hydrothermal systems. In: Hedenquist JW, Thompson JFH, Goldfarb RJ, and Richards JP (eds.) *100th Anniversary Volume of Economic Geology*, pp. 111–142. Littleton, CO: Society of Economic Geologists.

Hannington MD, Galley AG, Herzig PM, and Petersen S (1998) A comparison of the TAG mound and stockwork complex with Cyprus-type massive sulfide deposits. In: Humphris SE, Herzig PM, and Miller DJ (eds.) *Proceedings of the Ocean Drilling Program. Scientific Results*, vol. 158, pp. 389–415. College Station, TX: Ocean Drilling Program.

Hannington MD, Herzig PM, Scott S, Thompson G, and Rona PA (1991) Comparative mineralogy and geochemistry of gold-bearing sulfide deposits on the mid-ocean ridges. *Marine Geology* 101: 217–248.

Hannington MD, Jonasson I, Herzig P, and Petersen S (1995) Physical and chemical processes of seafloor mineralization at mid-ocean ridges. In: Humphris SE, Zierenberg RA, Mullineaux LS, and Thomson RE (eds.) *Seafloor Hydrothermal Systems: Physical, Chemical, Biological, and Geological Interactions, Geophysical Monograph Series*, vol. 91, pp. 115–157. Washington, DC: American Geophysical Union.

Hannington MD, Kjarsgaard I, and Bleeker W (1999a) Sulfide mineralogy, geochemistry, and ore genesis of the Kidd Creek deposit. Part II. The bornite zone. *Economic Geology Monograph* 10: 225–266.

Hannington MD, Poulsen KH, Thompson JFH, and Sillitoe RH (1999b) Volcanogenic gold in the massive sulfide environment. *Reviews in Economic Geology* 8: 319–350.

Hannington MD and Scott SD (1989) Gold mineralization in volcanogenic massive sulfides: Implications of data from active hydrothermal vents on the modern sea floor. *Economic Geology Monograph* 6: 491–507.

Hardardóttir V, Brown KL, Fridriksson Th, Hedenquist JW, Hannington MD, and Thorhallsson S (2009) Metals in deep liquid of the Reykjanes geothermal system, southwest Iceland: Implications for the composition of seafloor black smoker fluids. *Geology* 37: 1103–1106.

Harper GD (1999) Structural styles of hydrothermal discharge in ophiolite/seafloor systems. *Reviews in Economic Geology* 8: 53–73.

Hart T, Gibson HL, and Lesher CM (2004) Trace element geochemistry and petrogenesis of felsic volcanic rocks associated with volcanogenic Cu–Zn–Pb massive sulfide deposits. *Economic Geology* 99: 1003–1013.

Hekinian R, Fevrier M, Bischoff JL, Picot P, and Shanks WC (1980) Sulfide deposits from the East Pacific Rise near 21°N. *Science* 207: 1433–1444.

Holland HD (2004) The geologic history of seawater. In: Holland HD and Turekian KK (eds.) *Treatise on Geochemistry*, vol. 6, pp. 583–625. Oxford: Elsevier.

Holland HD (2005) Sedimentary mineral deposits and the evolution of Earth's near-surface environments. *Economic Geology* 100: 1489–1509.

Huston DL (1999) Stable isotopes and their significance for understanding the genesis of volcanic-hosted massive sulfide deposit: A review. *Reviews in Economic Geology* 8: 157–179.

Huston DL, Jablonski W, and Sie SH (1995a) The distribution and mineral hosts of silver in eastern Australian volcanogenic massive sulfide deposits. *The Canadian Mineralogist* 34: 529–546.

Huston DL and Large RR (1989) A chemical model for the concentration of gold in volcanogenic massive sulfide deposits. *Ore Geology Reviews* 4: 171–200.

Huston DL, Pehrsson S, Eglington BM, and Zaw K (2010a) The geology and metallogeny of volcanic-hosted massive sulfide deposits: Variation through geologic time and with tectonic setting. *Economic Geology* 105: 571–592.

Huston DL, Relvas JMRS, Gemmell JB, and Dreiberg S (2010b) The role of granites in volcanic-hosted massive sulphide ore-forming systems: An assessment of magmatic-hydrothermal contributions. *Mineralium Deposita* 46: 473–507.

Huston DL, Sie SH, Suter GF, Cooke DR, and Both RA (1995b) Trace elements in sulfide minerals from eastern Australian volcanic-hosted massive sulfide deposits: Part I. Proton microprobe analyses of pyrite, chalcopyrite, and sphalerite, and Part II. Selenium levels in pyrite: Comparison with δ^{34}S values and implications for the source of sulfur in volcanogenic hydrothermal systems. *Economic Geology* 90: 1167–1196.

Ishikawa Y, Sawaguchi T, Iwaya S, and Horiuchi M (1976) Delineation of prospecting targets for Kuroko deposits based on modes of volcanism of underlying dacite and alteration halos. *Mining Geology* 26: 105–117.

Janecky DR and Seyfried WE Jr. (1984) Formation of massive sulfide deposits on oceanic ridge crests: Incremental reaction models for mixing between hydrothermal solutions and seawater. *Geochimica et Cosmochimica Acta* 48: 2723–2738.

Kajiwara Y (1973) Chemical composition of ore-forming solution responsible for the Kuroko-type mineralization in Japan. *Geochemical Journal* 6: 141–149.

Kamenetsky VS, Binns RA, Gemmell JB, et al. (2001) Parental basaltic melts and fluids in eastern Manus backarc Basin: Implications for hydrothermal mineralization. *Earth and Planetary Science Letters* 184: 685–702.

Kasting JF, Howard MT, Wallmann K, Veizer J, Shields G, and Jaffrés J (2006) Paleoclimates, ocean depth, and the oxygen isotopic composition of seawater. *Earth and Planetary Science Letters* 252: 82–93.

Kelley DS and Delaney JR (1987) Two-phase separation and fracturing in mid-ocean ridge gabbros at temperatures greater than 700°C. *Earth and Planetary Science Letters* 83: 53–66.

Kelley DS and Früh-Green GL (2001) Volatile lines of descent in submarine plutonic environments: Insights from stable isotope and fluid inclusion analyses. *Geochimica et Cosmochimica Acta* 65: 3325–3346.

Kelley DS, Gillis KM, and Thompson G (1993) Fluid evolution in submarine magma-hydrothermal systems at the Mid-Atlantic Ridge. *Journal of Geophysical Research* 98: 19579–19596.

Knight CL (1957) Ore genesis – The source bed concept. *Economic Geology* 52: 808–818.

Knuckey MJ, Comba CDA, and Riverin G (1982) Structure, metal zoning, and alteration at the Millenbach deposit, Noranda, Quebec. In: Spence CD, Franklin JM, and Hutchinson RW (eds.) *Precambrian Sulfide Deposits, Geological Association of Canada Special Paper* 25, pp. 255–296. St. John's, NL: Geological Association of Canada.

Koschinsky A, Garbe-Schönberg D, Sander S, Schmidt K, Gennerich H-H, and Strauss H (2008) Hydrothermal venting at pressure-temperature conditions above the critical point of seawater, 5°S on the Mid-Atlantic Ridge. *Geology* 36: 615–618.

Large RR (1977) Chemical evolution and zonation of massive sulfide deposits in volcanic terrains. *Economic Geology* 72: 549–572.

Large RR (1992) Australian volcanic-hosted massive sulfide deposits: Features, styles, and genetic models. *Economic Geology* 87: 549–572.

Large RR, Doyle M, Raymond O, Cooke D, Jones A, and Heasman L (1996) Evaluation of the role of Cambrian granites in the genesis of world class VHMS deposits in Tasmania. *Ore Geology Reviews* 10: 215–230.

Large RR, McPhie J, Gemmell JB, Herrmann W, and Davidson GJ (2001) The spectrum of ore deposit types, volcanic environments, alteration halos, and related exploration vectors in submarine volcanic successions: Some examples from Australia. *Economic Geology* 96: 913–938.

Layton-Matthews D, Peter JM, Scott SD, and Leybourne MI (2008) Distribution, mineralogy, and geochemistry of selenium in felsic volcanic-hosted massive sulfide deposits of the Finlayson Lake district, Yukon Territory, Canada. *Economic Geology* 103: 61–88.

Lehman B (1991) Metallogeny of tin. In: Bhattacharji S, Friedman HJ, Neugebauer HJ, and Seilacher A (eds.) *Lecture Notes in Earth Sciences*, vol. 32. Berlin: Springer.

Lentz DR (1998) Petrogenetic evolution of felsic volcanic sequences associated with Phanerozoic volcanic-hosted massive sulfide systems: The role of extensional geodynamics. *Ore Geology Reviews* 12: 289–327.

Lesher CM, Goodwin AM, Campbell IH, and Gorton MP (1986) Trace element geochemistry of ore-associated and barren felsic meta-volcanic rocks in the Superior Province, Canada. *Canadian Journal of Earth Sciences* 23: 222–237.

Little CTS, Herrington RJ, Maslennikov VV, and Zaykov VV (1998) The fossil record of hydrothermal vent communities. In: Mills RA and Harrison K (eds.) *Modern Ocean Floor Processes and the Geological Record, Geological Society Special Publication* 148, pp. 259–270. London: Geological Society of London.

Lydon JW (1984) Volcanogenic massive sulphide deposits Part I: A descriptive model. *Geoscience Canada* 11: 195–202.

Lydon JW (1988) Volcanogenic massive sulphide deposits Part 2: Genetic Models. *Geoscience Canada* 15: 43–65.

Marumo K and Hattori KH (1999) Seafloor hydrothermal clay alteration at Jade in the back-arc Okinawa Trough: Mineralogy, geochemistry, and isotope characteristics. *Geochimica et Cosmochimica Acta* 63: 2785–2804.

Mercier-Langevin P, Hannington MD, Dubé B, and Bécu V (2010) The gold content of volcanogenic massive sulfide deposits. *Mineralium Deposita* 46: 509–539.

Miyashiro A (1973) The Troodos ophiolitic complex was probably formed in an island arc. *Earth and Planetary Science Letters* 19: 218–224.

Mosier DL, Singer DA, and Salem BB (1983) Geologic and grade-tonnage information on volcanic-hosted copper-zinc-lead massive sulfide deposits. US Geological Survey Open-File Report 83–89. Denver, CO: US Geological Survey.

Mottl MJ (1983) Metabasalts, axial hot springs, and the structure of hydrothermal systems at mid-ocean ridges. *Geological Society of America Bulletin* 94: 161–180.

Munha J, Barriga FJAS, and Kerrich R (1986) High ^{18}O ore-forming fluids in volcanic-hosted base metal massive sulfide deposits: Geologic, $^{18}O/^{16}O$, and D/H evidence from the Iberian pyrite belt, Crandon, Wisconsin, and Blue Hill, Maine. *Economic Geology* 81: 530–552.

Nisbet EG and Sleep NH (2001) The habitat and nature of early life. *Nature* 409: 1083–1091.

O'Neil JR and Taylor HP Jr. (1967) The oxygen isotope and cation exchange chemistry of feldspars. *American Mineralogist* 52: 1414–1437.

Oftedahl C (1958) On exhalative-sedimentary ores. *Geologiska Föreningens i Stockholm Förhandlingar* 80: 1–19.

Ohmoto H (1996) Formation of volcanogenic massive sulfide deposits: The Kuroko perspective. *Ore Geology Reviews* 10: 135–177.

Ohmoto H and Goldhaber MB (1997) Sulfur and carbon isotopes. In: Barnes HL (ed.) *Geochemistry of Hydrothermal Ore Deposits*, 3rd edn., pp. 517–612. New York: Wiley.

Ohmoto H, Mizukami M, Drummond SE, Eldridge CS, Pisutha-Arnond V, and Lenagh TC (1983) Chemical processes of Kuroko formation. *Economic Geology Monograph* 5: 570–604.

Ono S, Shanks WC III, Rouxel OJ, and Rumble D (2007) S-33 constraints on the seawater sulfate contribution in modern seafloor hydrothermal vent sulfides. *Geochimica et Cosmochimica Acta* 71: 1170–1182.

Paradis S, Taylor BE, Watkinson DI, and Jonasson IR (1993) Oxygen isotope zonation and alteration in the northern Noranda district, Quebec: Evidence for hydrothermal fluid flow. *Economic Geology* 88: 1512–1525.

Pearce JA, Alabaster T, Shelton AW, and Searle MP (1981) The Oman ophiolite as a Cretaceous arc-basin complex: Evidence and implications. *Philosophical Transactions of the Royal Society, Series A* 300: 299–317.

Peter JM and Goodfellow WD (2000) Mineralogy and bulk and rare earth element geochemistry of massive sulfide-associated hydrothermal sediments of the Brunswick horizon, Bathurst mining camp, New Brunswick. *Canadian Journal of Earth Sciences* 33: 252–283.

Peter JM and Goodfellow WD (2003) Hydrothermal sedimentary rocks of the Heath Steele belt, Bathurst mining camp, New Brunswick: Part 3: Application of mineralogy and mineral bulk compositions to massive sulfide exploration. *Economic Geology Monograph* 11: 417–433.

Piercey SJ (2010) An overview of petrochemistry in the regional exploration of volcanogenic massive sulphide (VMS) deposits. *Geochemistry: Exploration, Environment, Analysis* 10: 119–136.

Pisutha-Arnond V and Ohmoto H (1983) Thermal history, and chemical and isotopic compositions of the ore-forming fluids responsible for the Kuroko deposits in the Hokuroku district of Japan. *Economic Geology Monograph* 5: 523–558.

Potter RW and Brown DL (1977) The volumetric properties of aqueous sodium chloride solutions from 0°C to 500°C at pressures up to 2000 bars based on a regression of available data in the literature. *US Geological Survey Bulletin* 1421-C. Washington, DC: US Geological Survey.

Rasmussen B (2000) Filamentous microfossils in a 3235-million-year-old volcanogenic massive sulphide deposit. *Nature* 405: 676–679.

Richardson CJ, Cann JR, Richards HG, and Cowan JG (1987) Metal-depleted root zones of the Troodos ore-forming hydrothermal systems, Cyprus. *Earth and Planetary Science Letters* 84: 243–253.

Rimstidt JD (1997) Gangue mineral transport and deposition. In: Barnes HL (ed.) *Geochemistry of Hydrothermal Ore Deposits*, 3rd edn., pp. 487–516. New York: Wiley.

Roscoe SM (1965) Geochemical and isotopic studies, Noranda, and Matagami areas. *Canadian Institute of Mining and Metallurgy Bulletin* 68: 279–285.

Russell MJ, Hall AJ, Boyce AJ, and Fallick AE (2005) On hydrothermal convection systems and the emergence of life. *Economic Geology* 100: 419–438.

Rye RO (1993) The evolution of magmatic fluids in the epithermal environment: The stable isotope perspective. *Economic Geology* 88: 733–753.

Saccocia PJ, Ding K, and Berndt ME (1994) Experimental and theoretical perspectives on crustal alteration at mid-ocean ridges. In: Lentz D (ed.) *Alteration and Alteration Processes Associated with Ore-Forming Systems*, *Short Course Notes*, vol. 11, pp. 403–431. Canada: Geological Association of Canada.

Sangster DF (1968) Relative sulphur isotope abundances of ancient seas and strata-bound sulphide deposits. *Geological Association of Canada Proceedings* 19: 79–91.

Sangster DF (1972) Precambrian volcanogenic massive sulphide deposits in Canada – A review. *Geological Survey of Canada Paper* 72–22. Ottawa: Department of Energy, Mines and Resources.

Sangster DF and Scott SD (1976) Precambrian, strata-bound massive Cu–Zn–Pb sulfide ores in North America. In: Wolf KH (ed.) *Handbook of Strata-bound and Stratiform Ore Deposits*, vol. 7, ch. 5. pp. 129–222. London: Elsevier.

Sato T (1972) Behaviours of ore-forming solutions in seawater. *Mining Geology* 22: 31–42.

Schopf JW (1993) Microfossils of the Early Archean Apex chert: New evidence of the antiquity of life. *Science* 260: 640–646.

Scott SD (1997) Submarine hydrothermal systems. In: Barnes HL (ed.) *Geochemistry of Hydrothermal Ore Deposits*, 3rd edn., pp. 797–875. New York: Wiley.

Seward TM and Barnes HL (1997) Metal transport by hydrothermal ore fluids. In: Barnes HL (ed.) *Geochemistry of Hydrothermal Ore Deposits*, 3rd edn., pp. 435–486. New York: Wiley.

Seyfried WE Jr. (1987) Experimental and theoretical constraints on hydrothermal alteration processes at mid-ocean ridges. *Annual Review of Earth and Planetary Sciences* 15: 317–335.

Seyfried WE Jr. and Ding K (1993) The effect of redox on the relative solubilities of copper and iron on Cl-bearing aqueous fluids at elevated temperatures and pressures: An experimental study with application to subseafloor hydrothermal systems. *Geochimica et Cosmochimica Acta* 57: 1905–1917.

Seyfried WE Jr. and Ding K (1995) Phase equilibria in subseafloor hydrothermal systems: A review of the role of redox, temperature, pH, and dissolved Cl on the chemistry of hot spring fluids at mid-ocean ridges. In: Humphris SE, Zierenberg RA, Mullineaux LS, and Thomson RE (eds.) *Seafloor Hydrothermal Systems: Physical, Chemical, Biological, and Geological Interactions, Geophysical Monograph Series*, vol. 91, pp. 248–272. Washington, DC: American Geophysical Union.

Seyfried WE Jr., Ding K, Berndt ME, and Chen X (1999) Experimental and theoretical controls on the composition of mid-ocean ridge hydrothermal fluids. *Reviews in Economic Geology* 8: 181–200.

Seyfried WE Jr., Seewald JS, Berndt ME, Ding K, and Foustoukos DI (2003) Chemistry of hydrothermal vent fluids from the Main Endeavour Field, northern Juan de Fuca Ridge: Geochemical controls in the aftermath of June 1999 seismic events. *Journal of Geophysical Research* 108(B9): 2429.

Shanks WC III (2001) Stable isotopes in seafloor hydrothermal systems. *Reviews in Mineralogy and Geochemistry* 43: 469–526.

Shikazono N (2003) *Geochemical and Tectonic Evolution of Arc–Backarc Hydrothermal Systems and Implication for the Origin of Kuroko and Epithermal Vein-Type Mineralization and the Global Geochemical Cycle. Developments in Geochemistry*, vol. 8. Amsterdam: Elsevier.

Shock EL and Schulte MD (1998) Organic synthesis during fluid mixing in hydrothermal systems. *Journal of Geophysical Research* 103: 28513–28527.

Schulte M, Blake D, Hoehler T, and McCollom T (2006) Serpentinization and its implications for life on the early Earth and Mars. *Astrobiology* 6: 364–376.

Sillitoe RH, Hannington MD, and Thompson JFH (1996) High-sulfidation deposits in the volcanogenic massive sulfide environment. *Economic Geology* 91: 204–212.

Singer DA (1995) World-class base and precious metal deposits: A quantitative analysis. *Economic Geology* 90: 88–104.

Skirrow RG and Franklin JM (1994) Silicification and metal leaching in semiconformable alteration beneath the Chisel Lake massive sulfide deposit, Snow Lake, Manitoba. *Economic Geology* 89: 31–50.

Slack JF, Grenne T, Bekker A, Rouxel OJ, and Lindberg PA (2007) Suboxic deep seawater in the late Paleoproterozoic: Evidence from hematitic chert and iron formation related to seafloor-hydrothermal sulfide deposits, central Arizona, USA. *Earth and Planetary Science Letters* 255: 243–256.

Solomon M, Tornos F, Large RR, Badham JNP, Both RA, and Zaw Khin (2004) Zn–Pb–Cu volcanic-hosted massive sulphide deposits: Criteria for distinguishing brine-pool type from black smoker-type sulphide deposition. *Ore Geology Reviews* 25: 259–283.

Solomon M and Walshe JL (1979) The formation of massive sulfide deposits on the sea floor. *Economic Geology* 74: 797–813.

Spooner ETC, Chapman HJ, and Smewing JD (1977) Strontium isotopic contamination and oxidation during ocean floor hydrothermal metamorphism of the ophiolitic rocks of the Troodos Massif, Cyprus. *Geochimica et Cosmochimica Acta* 41: 873–890.

Spry PG, Peter JM, and Slack JF (2000) Meta-exhalites as exploration guides to ore. *Reviews in Economic Geology* 11: 163–201.

Stanton RL (1955) The genetic relationship between limestone, volcanic rocks, and certain ore deposits. *Australian Journal of Science* 17: 173–175.

Stanton RL (1960) General features of the conformable 'pyritic' orebodies. *Canadian Institute of Mining and Metallurgy Bulletin* 63: 22–27.

Stanton RL (1984) Observations on the Appalachian–Caledonide ore province and their influence on the development of stratiform ore genesis theory: A short historical review. *Economic Geology* 79: 1428–1441.

Stanton RL (1990) Magmatic evolution and the ore type-lava affiliations of volcanic exhalative ores. *Australasian Institute of Mining and Metallurgy Monograph* 14: 101–107.

Stanton RL (1994) *Ore Elements in Arc Lavas*. *Oxford Monographs on Geology and Geophysics*, vol. 29. London: Clarendon Press.

Thorpe RI (1999) The Pb isotope linear array for volcanogenic massive sulfide deposits of the Abitibi and Wawa subprovinces, Canadian Shield. *Economic Geology Monograph* 10: 555–576.

Trefry JH, Butterfield DB, Metz S, Massoth GJ, Trocine RP, and Feely RA (1994) Trace metals in hydrothermal solutions from Cleft segment on the southern Juan de Fuca Ridge. *Journal of Geophysical Research* 99: 4925–4935.

Turner JS and Campbell IH (1987) Temperature, density, and buoyancy fluxes in black smoker plumes and the criterion for buoyancy reversal. *Earth and Planetary Science Letters* 86: 85–92.

Urabe T (1974) Mineralogical aspects of the Kuroko deposits in Japan and their implications. *Mineralium Deposita* 9: 309–324.

Urabe T (1987) Kuroko deposit modeling based on magmatic hydrothermal theory. *Mining Geology* 37: 159–176.

Vearncombe S, Barley ME, Groves DI, McNaughton NJ, Mikucki EJ, and Vearncombe JR (1995) 3.26 Ga black smoker-type mineralization in the Strelley Belt, Pilbara Craton, western Australia. *Journal of the Geological Society* 152: 587–590.

Von Damm KL (1988) Systematics of and postulated controls on submarine hydrothermal solution chemistry. *Journal of Geophysical Research* 93: 4551–4561.

Von Damm KL (1990) Seafloor hydrothermal activity: Black smoker chemistry and chimneys. *Annual Review of Earth and Planetary Sciences* 18: 173–204.

Von Damm KL, Bischoff JL, and Rosenbauer RJ (1991) Quartz solubility in hydrothermal seawater: An experimental study and equation describing quartz solubility for up to 0.5 M NaCl solutions. *American Journal of Science* 291: 977–1007.

Wood SA, Crerar DA, and Borcsik MP (1987) Solubility of the assemblage pyrite-pyrrhotite-magnetite-sphalerite-galnea-Au-stibnite-bismuthinite-argentite-molybdenite in H_2O–CO_2–NaCl solutions from 200° to 350°C. *Economic Geology* 82: 1864–1887.

Wood SA and Samson IM (1998) Solubility of ore minerals and complexation of ore metals in hydrothermal solutions. *Reviews in Economic Geology* 10: 33–80.

Yang K and Scott SD (1996) Possible contribution of a metal-rich magmatic fluid to a seafloor hydrothermal system. *Nature* 383: 420–423.

Yang K and Scott SD (2002) Magmatic degassing of volatiles and ore metals into a hydrothermal system on the modern sea floor of the eastern Manus back-arc basin, western Pacific. *Economic Geology* 97: 1079–1100.

Yang K and Scott SD (2006) Magmatic fluids as a source of metals in arc/back-arc hydrothermal systems: Evidence from melt inclusions and vesicles. In: Christie DM, Fisher CR, and Lee S-M (eds.) *Back-Arc Spreading Systems: Geological, Biological, Chemical, and Physical Interactions*. *Geophysical Monograph Series*, vol. 166, pp. 163–184. Washington, DC: American Geophysical Union.

Zierenberg RA (1994) Sulfur content of sediments and sulfur isotope values of sulfide and sulfate minerals from Middle Valley. In: Mottl MJ, Davis EE, Fisher AT, and Slack JF (eds.) *Proceedings of the Ocean Drilling Program. Scientific Results*, vol. 139, pp. 739–748. College Station, TX: Ocean Drilling Program.